nature ecology & evolution

Supplementary information

https://doi.org/10.1038/s41559-025-02917-y

Sodium constraints on megaherbivore communities in Africa

In the format provided by the authors and unedited

Supplementary Information

Contents:

SUPPLEMENTARY TEXT

Text S1: Supplementary methods

S1.1 Mapping of foliar sodium concentration across sub-Saharan Africa

Foliar sodium observations:

We first collated observations of foliar sodium (Na) concentration throughout sub-Saharan Africa from available literature sources by systematically reviewing relevant papers in the ISI Web of Science and Google Scholar using combinations of the following keywords: [sodium, Na, concentration, plant, foliar, Africa] through June 2021. In total, we collated 596 observations from 16 published literature studies covering the time period 1963-2017 (for details of literature sources see our plant Na concentration database). We extended this dataset by adding 4,023 additional observations from measurements collected from various (n=18) field campaigns within sub-Saharan Africa over the period 1994-2021. Inevitably, there is some slight discrepancies between plant collection protocols across these field campaigns (e.g., targeting of specific plant species or leaf age). We therefore only included observations if foliar samples were healthy leaves that did not show obvious signs of herbivory or disease damage. Measurements were analysed for Na using an Inductively Coupled Plasma Optical Emission Spectrometer (ICP-OES), Inductively Coupled Plasma Mass Spectrometer (ICP-MS) or Horiba Compact Natrium Na Ion Meter LAQUAtwin readers in various labs in Africa, Europe and the USA. As with other studies collating data from multiple field campaigns and laboratories over long time periods (e.g., Kattge et al., 2021), there may have been small discrepencies between the laboratories and methodologies used to estimate foliar Na concentration. However, we are confident that such discrepancies do not impede our ability to analyse gradients across the continent that span >4 orders of magnitude (Extended Data Fig. 1).

In most cases, we obtained the raw data (i.e., one measurement per observation). However, in some circumstances (24 out of 289 locations), the data had already been pooled and only a mean value was available. As we wanted to maximise data inclusion and incorporate sites from across as much of the environmental space in sub-Saharan Africa as possible, in these instances, we randomly generated plant Na concentration values using the mean value obtained and the associated number of observations. At sites where we had a large sample size (n>20), the data was typically normally distributed, with a standard deviation approximately equal to the mean; where necessary, we therefore generated pseudo-data using a normal distribution around the mean-value obtained from

literature sources. This approach both allowed us to (i) maximise data inclusion and (ii) generate the median and 95th percentile estimates of foliar Na in each grid cell.

The taxonomic detail of reported foliar Na concentration measurements varied by field campaign/literature source. Where possible, we obtained the genus/species associated with individual measurements. However, this was only possible in 62% of cases. These observations were classified as belonging to either C_3 or C_4 plant functional groups using Osbourne et al. (2008). All other data were known to come from either grass, herb or woody plant groups. As the vast majority of herbs and woody plants in sub-Saharan Africa use C_3 photosynthetic pathways, and most grasses use C_4 photosynthetic pathways (Osbourne et al., 2008), we made the assumption that remaining herb and woody plant samples belonged to the C_3 functional group and remaining grasses to the C_4 functional group. For a small subset of observations (7.6%), it was unknown to which plant group (i.e., grass/herb/woody plant) samples belonged and these observations were removed from the dataset. Similarly, plants identified as using CAM photosynthesis were not included in this study.

Together, our final dataset comprised 4,258 measurements of foliar Na concentration collected over the period 1967-2018. Of this, 2,768 (65%) was from raw data, 1,490 (35%) from simulated data; 2,857 (67%) observations were from plants using the C_4 photosynthetic pathway and 1,401 (33%) using the C_3 photosynthetic pathway. For each photosynthetic pathway we then grouped all observations into 0.1-degree grid cells (~121 km^2), which resulted in 289 geographically distinct pooled grid-cell measurements (119 C_3 and 170 C_4). In each grid cell, we finally calculated the median and 95th percentile values that were used to train statistical models for predicting foliar Na concentration. To ensure that our approach of including simulated data in our final dataset did not influence the model predictions, we compared model predicitons using raw data only and raw and simulated data together. For both the median and 95th percentile models, the inclusion of simulated data did not alter overall model performance, variable importance rankings or relationships between variables and foliar Na concentrations assessed by partial dependence plots.

<u>Predictor variables generated in this study to predict foliar Na concentration:</u>

A: Sodium aerosol deposition

Sodium aerosol deposition was estimated using an ensemble of ten independent sea salt aerosol deposition model outputs from the Aerosol Comparisons between Observations and Models Phase II project (AeroCom; <u>https://aerocom.met.no/Welcome.html</u>). These models have been well validated

(Tsigaridis et al., 2014) and a full list of models used for this ensemble is presented in Fig. S3. All model simulations were run for the year 2006 at a 1°x1° resolution. Consequently, to remove large step changes in neighbouring grid cells located close to the coast, we smoothed the output to a 0.1° x 0.1° resolution using bilinear interpolation. Finally, we converted sea salt aerosol deposition to sodium aerosol deposition using equation S1, based on the ratio of sodium within sea salt aerosol from Vet et al. (2014).

$$Na_{dep} = 0.307 * SSA_{dep} \qquad \text{(equation S1)}$$

where Na_{dep} is sodium aerosol deposition in kg km^{-2} yr^{-1} and SSA_{dep} is sea salt aerosol deposition in kg km^{-2} yr^{-1}. To validate our sodium aerosol deposition outputs, we compared modelled monthly and annual wet deposition rates to empirical data collected at 11 sites distributed across sub-Saharan Africa as part of the International Network to study Deposition and Atmospheric chemistry in Africa (INDAAF; https://indaaf.obs-mip.fr/network/). At each site, rainwater chemistry has been collected and analysed for chemical constituents. The mean number of years over which data was collected at each site was 9.7±5.4 years. In general, there is good agreement between modelled and empirical estimates of wet sodium aerosol deposition (Fig S2b). This is especially the case in sites with very high (e.g. Cape Point, South Africa) and very low (e.g. >100km inland) sodium deposition. However, three sites located in southern Africa are overestimated, indicating discrepancies between model and empirical estimates in some locations. As we used the model results for estiming sea salt deposition at each plant observation (see below), future efforts to quantify wet sodium deposition fluxes will benefit from ascertaining why these three sites differed. Dry aerosol deposition is harder to estimate as it is a function of particle size, surface roughness, ambient climate conditions and wind speed (Adon et al., 2013; Zhang and He, 2014). Therefore, we did not validate this component of sodium aerosol deposition. At the 11 INDAAF sites, dry deposition was modelled between 5-2000% of the wet component, indicating that in some places modelled dry deposition forms a substantial component of the total aerosol sodium deposition flux.

B: Sodium rock weathering

Mineral weathering in soils is mediated by temperature, water flows and soil pH, partly controlled by plants and associated organisms during nutrient uptake. To estimate the release of Na from soil minerals, we used a chemical weathering model (Taylor et al., 2016), which calculates mineral dissolution rates as affected by plant productivity and soil moisture from the Sheffield Dynamic Global Vegetation Model (Woodward and Lomas, 2004). The models were forced with CRU TS v. 3.00 climate

data (Harris et al., 2014). We calibrated the weathering model using measured elemental concentrations and inorganic carbon fluxes in river waters (Gaillardet et al., 1999).

C: Net primary productivity

Mean annual net primary productivity (NPP) was calculated over the period 2001-2010 using the Moderate Resolution Imaging Spectroradiometer (MODIS) annual NPP MOD17A3HGF V6 product at a resolution of 500m. This time period was selected as it encompasses the majority of empirical foliar sodium concentration measurements collated for this study. Data were extracted using the Google Earth Engine platform (https://earthengine.google.com/).

S1.2 Large mammalian herbivore fecal sample collection and analysis (this study)

We collected fresh fecal samples (determined by direct observation of animals) between 2017-2021 from ten wildlife reserves in southern Africa, where foliar Na concentration shows strong coast – inland gradients (n=891; Extended Data Fig. 1; Fig. 1). Additional unpublished data (n=146) had already been collected in Laikipia (Kenya) in 1998-2000, Hluhluwe – Imfolozi Game Reserve (South Africa) in 2018 and Gorongosa (Mozambique) in 2021-2022. All samples were collected as fresh single faecal samples from one individual. Specific locations of all fecal collections in our final database are outlined in Table S3. South African samples specifically collected for this project were collected fresh and frozen within 8 hours at -20^{o}C. Samples were transported to the Endocrine Research Laboratory, University of Pretoria, for lyophilisation at -54^{o}C and ~0.96 mbar for 5-7 days until completely dry. Dry fecal samples were subsequently pulverised using a pestle and mortar to homogenise the sample. At the University of Pretoria Soil Sciences Laboratory, 0.25-0.30g of dried fecal sample was digested in 10ml of Suprapur Nitric acid (65%) and analysed for Na concentration using a SPECRO GENESIS Inductively coupled plasma optical emission spectrometer (ICP-OES). Samples from Hluhluwe – Imfolozi Game Reserve (South Africa), Gorongosa (Mozambique) and Laikipia (Kenya) were analysed using an Inductively coupled plasma mass spectrometer (ICP-MS). These original data were added to 319 observations from six peer-reviewed publications (Table S3) for a final dataset of 1,356 observations from 28 large herbivore species. The large-herbivore species from which we obtained faecal Na observations are outlined in Table S4.

S1.3 Variables considered for predicting large herbivore density across sub-Saharan Africa

To understand the effect of sodium availabaility on large herbivore density across sub-Saharan Africa, we fitted generalized additive mixed models (GAMMs). This followed a similar approach to model mammal density (e.g., Santini et al., 2022), but with modifications, outlined in the methods section of the main text. We considered numerous functional trait, environmental, and anthropic factors but only included a subset to prevent model overfitting and interpretability. Below we provide an overview of these to provide context for the inclusion of our final eleven fixed effect predictors.

Functional trait variables:

Following Santini et al. (2022) we included functional traits of body mass and diet (e.g., % omnivory) as these were found to be the major determinants of mammal density. Body mass was taken from Hempson et al. (2015) and % omnivory was taken from Elton Traits v1.0 (Wilman et al., 2014). We also included habitat preference; a categorical variable with three levels from Hempson et al. (2015), and applied to the vegetation map of White (1983).

Environmental variables:

For environmental variables, we generated proxies of forage and water availability, as these have been shown to influence herbivore densities along resource gradients (Coe et al. 1976; Bell, 1984; East 1984; fritz and Duncan, 1997; Hempson et al., 2015; Pranzini et al., 2024). For total forage availability we used NDVI, for forage seasonality we used precipitation concentration index (a measure of how concentrated rainfall is throughout the year) and forage quality was assumed related to soil fertility. Water availability was measured as average distance to nearest permanent water source. Details of our proxies used for environmental variables are provided in Table S5.

We calculated dietary sodium availability for both unselective and selective scenarios using equation 1 and extracting sodium concentration from the appropriate C_3 and C_4 maps and percentage C_4 grasses taken hierarchically from (1) Pansu et al. (2022), (2) Kartzinel and Pringle (2020), (3) new data from R.M. Pringle et al., (4) Sponheimer et al. (2003), (5) Codron et al. (2007), (6) Cerling et al. (2003). For the 18 species not found in refs 1-6, we approximated dietary C_4% based on categories from (7) Hempson et al. (2015; see also Gagnon & Chew 2000), where browsers (BRW) and frugivores (FRG) are equal to 0%, browser-grazer intermediates (BGI) and generalists (GEN) are equal to 50%, variable grazers (GRV) are equal to 75%, and obligate grazers (GRO) are equal to 100%.

The new dietary C_4 % data provided by R.M. Pringle et al., were for six species of West African forest ungulates and analysed using fecal DNA metabarcoding. The laboratory, sequencing, and

bioinformatic protocols that used here match those used by Pansu et al. (2022) and are described comprehensively in the main text and supplementary information of that work. We provide a brief synopsis to contextualize the contents of the data file but refer readers to Pansu et al. (2022) for details. Fresh fecal samples were collected from August–October 2021 during walking surveys led by Dr. Lotanna Micah Nneji in national parks in Nigeria and Cameroon. Homogenized subsamples were suspended in in lysis buffer and exported to Princeton University. Sample collection and shipping protocols were in accordance with permits from Nigeria's National Park Service, Cameroon's Ministries of Scientific Research and Innovation and Forestry and Wildlife, and the United States Department of Agriculture's Animal and Plant Health Inspection Service. Provisional mammal identifications made in the field were confirmed, or updated when necessary, by sequencing a fragment of the mitochondrial 16S gene. For diet analysis, we amplified the plant chloroplast *trn*L-P6 marker and sequenced libraries on a high-throughput platform. To estimate proportional grass consumption for each sample (individual), we rarefied the sequence data to 1500 reads and excluded any sequences that accounted for less than 1% of reads; we then summed the number of reads identified as grasses (family Poaceae) and divided by the rarefied read depth to obtain a proportion.

Anthropogenic variables:

We considered eight anthropogenic variables that have previously been shown to influence large herbivore density in Africa (Benitez-Lopez et al., 2017; Kuiper et al., 2023; Pranzini et al., 2024; Fa et al., 2022). We split these into five potential axes of human influence: (1) human accessibility, (2) hunting/poaching motivation, (3) herbivore protection and security, (4) herbivore hunting pressure and (5) broader ecosystem modifications.

- **Human accessibility:**
    - Distance to nearest city → Rationale: easier access to protected areas via reduced travel time for poaching/hunting groups (Critchlow et al., 2015; Schlossberg et al., 2020); extracted from Nelson et al. (2019).
    - Rural density → Rationale: direct and indirect influence of humans, including bushmeat hunting, increases with increasing density; we followed Prazini et al. (2024) and extracted rural density from Gridded Population of the World, Version 4 (GPWv4) at 50x50km resolution.

- **Human motivation:**

- Household wealth → Rationale: socio-economic conditions that represent poverty may encourage individuals to engage in poaching/hunting for protein or income (Duffy & St John, 2013); extracted International Wealth Index (IWI) from the Global Data Lab: https://globaldatalab.org/iwi/ (Smits and Steendijk, 2015). We used a mean value from the period 1992-2010 coincident with large herbivore density measurements.
- Human development → Rationale: communities that are impoverished may be more likely to participate or facilitate poaching/hunting for protein or income (Cooney et al., 2016); extracted Human Development Index (HDI) from the Global Data Lab: https://globaldatalab.org/shdi/ (Smits and Permanyer, 2019). We used a mean value from the period 1992-2010 coincident with large herbivore density measurements.

- **Large herbivore protection and security:**
  - Governance → Rationale: poor governance (corruption) may facilitate poaching/illegal hunting in protected areas (Smith et al., 2003); extracted from World Bank's World Governance Index: https://www.worldbank.org/en/publication/worldwide-governance-indicators/interactive-data-access (Kaufman et al., 2011).
  - Deaths due to armed conflict → Rationale: more intense armed conflict may lead to institutional and socioeconomic conditions that facilitate poaching/illegal hunting in protected areas (Gaynor et al., 2016; Daskin and Pringle, 2018); following the methods of Kuiper et al. (2023) and Daskin and Pringle (2018) we sourced data from The Uppsala Conflict Data Program (UCDP): https://ucdp.uu.se/downloads/index.html#ged_global and summed all conflict between 1989-2010.

- **Large herbivore hunting threat**:
  - Hunting → Rationale: high levels of hunting may reduce herbivore density below the ecosystem carrying capacity; spatially explicit, species-specific hunting pressure layers are not available, we therefore extracted the community-level hunting layer for mammals generated by Harfoot et al. (2021) Figure 3c. This map provides a standardized proportion of mammal species within a community that may be targeted for hunting.

- **Broader ecosystem modifications**:
    - Human modification index → Rationale: changes of the ecosystem via anthropogenic modifications (e.g., land use change, logging) may reduce or increase the ecosystem carrying capacity; we considered the human modification layer of (Kennedy et al., 2019).

- **Unaccounted anthropogenic effects:**
    - Region → Rationale: to account for historical and socio-economic anthropogenic factors not captured by the fixed effects. Split into west, central, east and southern Africa.

There was, however, substantial correlation between some anthropogenic factors. To ensure interpretability, we subset the full suite of considered anthropogenic factors, aiming to maximise the various axis of potential human impact on herbivore density (accessibility, motivation, protection, etc). The final anthropogenic factors that we included in our models were: (1) **Accessibility**: Distance to city, (2) **Motivation/Herbivore protection**: Human Development Index (closely correlated with International Wealth Index and Governance), (3) **Direct and indirect impact**: Hunting pressure (correlated with rural density, armed conflict, and human modification), (4) **Region:** to account for historical and socio-economic factors not captured by anthropogenic fixed effects.

The final eleven fixed effect variables and two random effect variables included in our statistical modelling approach are listed in Table S5.

Text S2: Supplementary results

Foliar sodium concentration models

The ensemble model was consistently the best model, although the predictive power of all models decreased with distance from the training point. With the full dataset, the ensemble model had an R^2 of 0.35-0.4 in both the median and 95th percentile scenarios; the root mean squared error (RMSE) was low (< 0.4 log_{10} units) demonstrating that the model can accurately predict within half an order of magnitude. The individual machine learning methods demonstrated variable predictive power, although the neural nertwork was consistently the poorest performing model. When predicting foliar Na concentration in areas far from the training points, model performance was poor across models with a low R^2 <0.2 and a RMSE >0.7 log_{10} units. Nevertheless, the ensemble model was still better than our two baseline models (i) sea salt aerosol deposition rate, and (ii) a purely spatial model generated by using a kernel density smoother between geographic points. The R^2 of these models were 0.15-0.3, respectively for the full dataset, decreasing to 0.1-0.15 when nearby points were removed. The corresponding RMSE values were ~0.6 log_{10} units. As a result, the inclusion of environmental covariates improves our ability to map foliar Na concentrations at continental scales.

Large-herbivore density models

For all generalized additive mixed models (GAMMs) fitted in this study, we first checked model diagnostics – including concurvity and spatial autocorrelation – to ensure that our models were not overfitted and robust for prediction. Concurvity did not exceed >0.8 in any model – a measure of co-linearity in GAMMs, where values >0.8 should be treated with caution due to reduced interpretability (Pedersen et al., 2019). Absence of spatial autocorrelation was confirmed using variograms and the calculation of Moran's I statistic. For the GAMM fitted to density data of all herbivores there was no evidence of spatial autocorrelation in the variogram (Fig. S9), and the Moran's I test confirmed the absence of spatial autocorrelation effects on the residuals (Observed = -0.00059; Expected = -0.00085; Variance = 0.0000016; p-value = 0.42). Similarly, for the GAMM fitted to density data for megaherbivores only there was no evidence of spatial autocorreolation in the variogram (Fig. S9), and the Moran's I test confirmed the absence of spatial autocorrelation effects on the residuals (Observed = -0.0112; Expected = -0.00746; Variance = 0.000093; p-value = 0.65).

To check the robustness and predictive performance of our model we used spatial-block, taxonomic-block and random-block cross validation (Roberts et al., 2017). For spatial-block cross validation we used the 'spatialsample' R package (Roberts et al., 2017) and split our data into 3x3 degree geographical blocks and grouped the blocks into 10-folds. The size of these blocks ensures spatial independence and avoids training of data that overlap spatially with those used for testing (Santini et al., 2022). Taxonomic blocking was applied to each species iteratively. For random-block cross validation we randomly split the data into 70% training and 30% testing, and repeated this procedure 10 times. For each cross validation exercise, we reported the mean ± standard deviation of the R^2 and RMSE across folds or species, respectively. We reported performance metrics for both the training dataset and the test dataset, where a large drop in predictive performance indicates model overfitting.

The performance of our all-herbivore model on the test datasets in each cross validation exercise was generally decent, with mean R^2 values across folds/species between 0.2-0.3 and mean RMSE values of 0.76-0.84. However, there was large variation of predictive performance between species in the taxonomic cross validation (Table S6), highlighting that our model doesn't capture species-level dynamics, which are instead incorporated into species random effects. This is likely because we reduced the number of species-specific trait variables (e.g., diet, gut physiology) in our model to prevent model overfitting. There is an expected decrease in model performance between the training and test dataset, suggesting that the model may be slightly overfit. However, the consistency of predicted vs observed points close to the 1:1 line across folds in the spatial-block and random-block cross validation gives confidence that the predictive performance is robust (Fig. S10). As a result, our all-herbivore model is more robust for analysing patterns in space, but less robust for species-specific deviations from these trends.

For the megaherbivore-only model we only performed spatial-block and random-block cross validation as there were only four species for taxonomic-block. The mean performance metrics for both spatial-block and random-block cross validation was better in the megaherbivore-only model than the all-herbivore model, but with a greater standard deviation between folds (Table S6). This indicates that the model may be more overfit; however, this is expected to a degree as the megaherbivore model has many fewer observations (n=135) compared to the full dataset (n=1170). Again, the consistency of model prediction to the 1:1 line between predicted and observed points gives confidence that the model is generally robust for predicting patterns in space (Fig. S10).

Text S3: Supplementary discussion

Alternative sources of herbivore sodium intake

One factor we did not address is the potential for herbivores to compensate for Na deficiency via geophagy. The primary element with elevated concentrations in soils consumed by large herbivores at mineral licks in multiple grassland and savanna ecosystems is Na (Tracy et al. 1995; Holdo et al. 2002; Kalumanga et al. 2016). Nevertheless, while geophagy may help alleviate Na deficiency in large herbivore diets, this activity could still incur energetic costs associated with finding and moving to Na-enriched mineral licks, could limit herbivore distribution in portions of the landscape distant from licks, and could induce costs associated with consumption of toxic levels of other minerals, such as Al (Tracy et al. 1995). We note that in regions where dietary [Na] was <500 mg/kg (unselective feeding scenario), fecal [Na] varied much more widely (from 30 to 3,000 mg/kg) than in regions where dietary [Na] exceeded 500 mg/kg (Fig. 2a). Geophagy may be one factor enabling herbivore fecal [Na] to occasionally reach high levels (e.g. >1,000 mg/kg) in regions with deficient [Na] in forage. At the same time, a substantial proportion of herbivore fecal samples collected in regions with Na-deficient forages contained < 300 mg/kg Na (Fig. 2a), consistent with the idea that geophagy does not generally compensate for Na-deficient forage across species.

Modelling limitations and future improvements

The foliar sodium concentration maps generated for this study represent the first attempt to map the availability of herbivore dietary sodium at continental scales. However, there were a number of inevitable limitations in our capacity to model foliar Na concentrations:

Spatial data availability: There are large areas of sub-Saharan Africa (41%) that are >500 km from the nearest plant functional group data point (Extended Data Fig. 2). While inspection of partial dependence plots from the machine learning techniques used to generate these maps generally reveal logical outcomes, future mapping efforts will benefit from the addition of new data that represent a broader area. In particular, the Horn of Africa, Congo rainforest, and coastal west Africa are currently poorly represented, both in this study and the vast majority of ecological research in Africa (Pringle et al., 2023). Our maps were generated at 0.1 degree resolution; however this overlooks fine-scale gradients that occur within local landscapes (e.g., around natural mineral licks, or between geological strata). The coarseness of our maps partly reflects the available resolution of our predictor variables

(e.g., rock weathering inputs; see Table S1) and the scale of our herbivore density data. Improvements in the resolution of field and remotely-sensed data will help refine further iterations of the maps we present here.

Temporal data availability: Our study only provides a single snapshot in time for foliar Na concentrations. Yet, our dataset for foliar Na concentration spanned from 1963-2018, while our faecal dataset spanned from 1989 to 2021 (Fig. S7). This may lead to incongruities between the maps we generated to estimate forage Na and predict faecal Na (Fig 2; Extended Data Fig. 5). To check if there are major changes in foliar Na concentrations through time, we regressed foliar Na with sample year for regions of Africa banded into sea salt aerosol depositon bins (Fig S7). This plot revealed that the majority of variance in foliar Na is explained by other factors (e.g., spatial, phylogenetic). However, while there is not an obvious trend of decreasing foliar Na through time and thus any temporal component is not likely to significantly impact our assessment of foliar Na impact as a driver of faecal Na at the continental scale, more rigorous analysis may elucidate temporal patterns. For example, assessment of how seasonal and inter-annual factors (including episodic extreme events such as droughts and cyclones) influence fluctuations in local Na availability will enable assessment of how fine-grained spatio-temporal variation affects herbivore density and movement patterns (Borer et al., 2019; Vogel et al., 2020). Similarly, expansion of the current database may reveal if there have been changes in Na availability over time due to CO_2-induced nutrient dilution (Kaspari and Welti, 2025).

Species-level data availability: Our modelled estimates of herbivore density do not include herbivore-specific differences in Na demand or the availability of alternative sodium sources (e.g. geophagy, osteophagy, omnivory; Holdo et al., 2002; Rothman et al., 2006; Clay et al., 2017). Species-specific differences in Na requirement are essentially unknown. Body mass is one known covariate (Duvall et al., 2023), with estimated Na requirement scaling to the power of 0.91, but there is considerable variation in this relationship (95% CI of the scaling exponent: 0.80 – 1.00) some of which is undoubtedly explained by other physiological factors that influence sodium needs and conservation. Adding these factors may help improve the relationships between modelled dietary sodium and both fecal Na concentration and herbivore density.

Missing covariates: Statistical modelling of animal density at continental-scales generally cannot account for factors that can be pivotal limiting factors of realized densities at local scales. Future attempts will likely benefit from the inclusion of additional covariates (e.g., impacts of humans and

other predators, along with other dimensions of forage quality that are known to be important, such as protein and digestibility; Suttle et al., 2010).

Modelling protocols: In our approach, we generated predictions of foliar Na concentration using a suite of predictor variables. We then used these model predictions to estimate how plant Na availability may influence large-herbivore density. Inevitably such an approach risks undetectable correlation or "double counting" (i.e., variables used to predict foliar Na may be related directly to herbivore density). In general, however, our variables used for modelling foliar Na concentration had low correlation coefficients (<0.3); those that had high correlation coefficients (e.g., NDVI, NPP, Aridity) were either explicitly included in our model to predict herbivore density or had negative relationships with foliar Na concentrations. Importantly, this provided an opportunity to tease apart the effects of Na and total forage availability in shaping herbivore communities at the continental scale as the limiting mechanism (i.e., not enough forage or Na) were opposed to each other. Nevertheless, future studies that directly measure forage mineral availability *in-situ* alongside associated herbivore densities will help overcome the problems of using modelled data rather than direct empirical measurements.

SUPPLEMENTARY TABLES

Table S1. Predictor variables and associated details used to model foliar Na concentration.

Mechanism	Predictor	Variable importance code	Data source	Units	Resolution (m)	Dataset range		Sampled range		Reference
						Min	Max	Min	Max	
Input	Sea salt aerosol deposition	SSA	AeroCom2	kg Na km^{-2} yr^{-1}	~10000	3.0	516.1	3.5	322.3	*This study – see SI text for further information*
	Rock sodium weathering rate	Weathering	Taylor et al. (2016)	NA	~50000	1.0	7.1	1.0	6.7	*This study – see SI text for further information*
	Alluvial %	Alluvial	USGS Ecosystems project	%	250	0.0	1.0	0.0	1.0	Sayre et al. (2013)
	Height Above Nearest Drainage	HAND	SRTM-30	m	30	0.0	1133.9	2.5	155.8	Donchyts et al. (2016)
Retention	Aridity index	Aridity	WorldClim2	NA	1000	0.0	3.1	0.0	2.2	Trabucco and Zomer (2018)
	Soil clay fraction	Clay	SoilGrids250	%	250	3.6	65.5	9.1	53.3	Hengl et al. (2015)
	Cation exchange capacity	CEC	SoilGrids250	cmol kg^{-1}	250	1.7	67.1	4.4	44.7	Hengl et al. (2015)
Uptake	Exchangeable soil Na (20-50cm)	Ex_Na	SoilGrids250	cmol kg^{-1}	250	0.0	40.1	0.1	9.5	Hengl et al. (2015)
	Exchangeable soil K (20-50cm)	Ex_K	SoilGrids250	cmol kg^{-1}	250	0.0	4.6	0.1	4.4	Hengl et al. (2015)
	Soil pH	pH	SoilGrids250	NA	250	4.4	9.4	4.9	8.6	Hengl et al. (2015)
Dilution	Net primary productivity	NPP	MODIS	kg C m^{-2} yr^{-1}	500	0	2.3	0	1.8	*This study – see SI text for further information*

Table S2: Hyperparameter grids used to train foliar sodium concentration predictive models.

Model	Parameter		Parameter value sequence		
	Name	Details	Min	Max	By
Gradient boosting machine (GBM)	interaction.depth	complexity of tree	1	5	2
	n.trees	number of iterations	0	2500	50
	shrinkage	learning rate	0.001	0.01	NA
	n.minobsinnode	minimum number of nodes to commence splitting	NA	10	NA
Random forest (RF)	mtry	number of randomly selected predictors	1	11	1
Neural network (NNET)	size	number of hidden units	1	50	5
	decay	weight decay	0	1	0.05
Support vector machine (SVMRADIAL)	C	cost	0	1	0.25
	sigma	sigma	0.5	2	0.5
CUBIST	committees	number of committees	1	100	5
	neighbours	number of instances	1	8	1

Table S3: Site and collection details for herbivore fecal samples. Total n=1,356 fecal samples. In some instances, literature sources presented fecal concentration values as the mean across several individual samples. In these cases, we considered the combined sample as an individual measurement.

Country	Wildlife area	Lat	Lon	Modelled foliar Na concentration (mg kg^{-1}; C_3 median – C_4 95th)	n	Anthropogenic mineral lick provision	Source
Kenya	Laikipia	0.3	36.9	172-564	146	No	This study
	Mt Kenya	-0.2	37.2	219-609	15	No	Mahney and Hancock (1990)
Mozambique	Gorongosa	-18.8	34.5	228-2993	86	No	This study
South Africa	andBeyond Phinda Private Game Reserve	-27.8	32.4	1130-6657	53	No	This study
	Balule Private Game Reserve	-24.4	30.9	181-717	29	No	This study
	Hluhluwe – Imfolozi Game Reserve	-28.1	32.1	690-8591	75	No	This study
	Kariega	-33.6	26.6	1045-3947	60	No	This study
	Kruger National Park	-22.7	31.0	175-472	10	No	Macandza et al. (2014)
	Kruger National Park	-24.5	31.5	277-687	53	No	Yoganand and Owen-Smith (2014)
	Manyeleti Nature Reserve	-24.6	31.5	322-1136	108	No	This study
	Nylsvley Nature Reserve	-24.7	28.7	214-1181	2	Unknown	Dörgeloh et al. (1998)
	Palabora	-24.0	31.2	239-380	94	Unknown	Sach et al. (2020)
	Percy Fyfe Nature Reserve	-24.0	19.2	262-639	1	Unknown	Dörgeloh et al. (1998)
	Samara Private Game Reserve	-32.5	24.9	219-563	39	No	This study
	Sibuya Private Game Reserve	-33.6	26.7	1274-3581	59	No	This study
	Skuinsdraai	-24.8	29.36	212-649	1	Unknown	Dörgeloh et al. (1998)
	Thanda Private Game Reserve	-27.7	32.0	1354-6072	67	No	This study
	Tswalu Kalahari Private Game Reserve	-27.2	22.3	111-584	315	Yes	This study
Zimbabwe	Hwange National Park	-18.8	26.8	164-1059	138	No	Holdo et al. (2002)

Table S4: Summary of traits for 65 large herbivore species >2kg included in generalised additive mixed-effect models (GAMMs) predicting herbivore density across sub-Saharan Africa, including number of density observations for each species. Data for 27 extant species are not included as no density information were available for these species. Functional traits of body mass, gut physiology, and surface-water requirement are included from Hempson et al. (2015). For surface-water requirement; 0 = none, 1 = low, 2 = high. Percent grass consumption or dietary % C_4 were taken hierarchically from (1) Pansu et al. (2022), (2) Kartzinel and Pringle (2020), (3) data from R.M. Pringle et al., (4) Sponheimer et al. (2003), (5) Codron et al. (2007), (6) Cerling et al. (2003). For the 18 species not found in refs 1-6, we approximated dietary C_4% based on categories from (7) Hempson et al. (2015; see also Gagnon & Chew 2000), where browsers (BRW) and frugivores (FRG) are equal to 0%, browser-grazer intermediates (BGI) and generalists (GEN) are equal to 50%, variable grazers (GRV) are equal to 75%, and obligate grazers (GRO) are equal to 100%. Omnivory % was defined as all non-plant dietary resources taken from Elton Traits v1.0 (Wilman et al., 2014).

Species	Common name	n density obs	Body mass (kg)	Gut physiology	Water req	Dietary C_4 %	C4 ref	Omnivory %	Faecal collect
Aepyceros melampus	Impala	40	49.1	ruminant	2	26.5	1	0	Y
Alcelaphus buselaphus	Hartebeest	65	150.3	ruminant	2	71.0	1	0	Y
Antidorcas marsupialis	Springbok	20	35.3	ruminant	1	23.0	4	0	Y
Cephalophus dorsalis	Bay duiker	1	20.6	ruminant	0	0.0	3	10	N
Cephalophus natalensis	Red forest duiker	3	11.9	ruminant	0	1.5	4	10	N
Cephalophus niger	Black duiker	2	21.0	ruminant	0	0.0	7	10	N
Cephalophus ogilbyi	Ogilby's duiker	1	19.0	ruminant	0	0.0	3	10	N
Cephalophus rufilatus	Red-flanked duiker	13	10.2	ruminant	0	0.0	7	10	N
Cephalophus silvicultor	Yellow-backed duiker	4	62.7	ruminant	0	0.0	3	10	N
Cephalophus zebra	Zebra duiker	1	16.9	ruminant	0	0.0	7	10	N
Ceratotherium simum	White rhino	8	2195.8	non-ruminant	2	82.0	1	0	Y
Connochaetes gnou	Black wildebeest	8	142.7	ruminant	2	94.0	4	0	N
Connochaetes taurinus	Blue wildebeest	34	220.1	ruminant	2	79.0	1	0	Y
Damaliscus lunatus	Topi	32	126.7	ruminant	1	78.5	1	0	N
Damaliscus pygargus	Bontebok	10	68.4	ruminant	2	90.0	4	0	N
Diceros bicornis	Black rhino	17	999.9	non-ruminant	2	8.0	1	0	Y
Equus grevyi	Grévy's zebra	3	400.2	non-ruminant	1	98.0	1	0	N
Equus quagga	Plains zebra	40	280.4	non-ruminant	2	91.0	1	0	Y
Equus zebra	Mountain zebra	12	278.5	non-ruminant	2	75.0	7	0	Y
Eudorcas albonotata	Mongalla gazelle	2	19.0	ruminant	0	75.0	7	0	N
Eudorcas rufifrons	Red-fronted gazelle	2	26.1	ruminant	1	50.0	7	0	N
Eudorcas thomsonii	Thomson's gazelle	3	19.0	ruminant	1	48.0	1	0	N
Giraffa camelopardalis	Giraffe	49	1117.5	ruminant	1	0.5	1	0	Y
Hippopotamus amphibius	Hippopotamus	29	1866.9	non-ruminant	2	60.5	1	0	N
Hippotragus equinus	Roan antelope	48	264.0	ruminant	2	26.0	1	0	Y
Hippotragus niger	Sable antelope	21	210.5	ruminant	2	90.0	1	0	Y
Hyemoschus aquaticus	Water chevrotain	2	11.1	ruminant	0	50.0	7	0	N

Hylochoerus meinertzhageni	Giant forest hog	2	157.7	non-ruminant	2	50.0	7	0	N
Kobus ellipsiprymnus	Waterbuck	62	211.8	ruminant	2	32.0	1	0	Y
Kobus kob	Kob	28	73.1	ruminant	2	95.0	6	0	N
Kobus leche	Red lechwe	7	89.2	ruminant	2	62.0	0	0	N
Kobus vardonii	Puku	5	70.1	ruminant	2	60.0	1	0	N
Litocranius walleri	Gerenuk	5	39.1	ruminant	0	5.0	2	0	N
Loxodonta africana	Elephant	61	4101.8	non-ruminant	2	33.0	1	0	Y
Madoqua guentheri	Günther's dik-dik	2	4.1	ruminant	0	1.5	1	0	N
Madoqua kirkii	Kirk's dik-dik	1	5.6	ruminant	0	0.0	6	0	Y
Nanger granti	Grant's gazelle	10	57.4	ruminant	0	16.0	1	0	N
Nanger soemmerringii	Soemmerring's gazelle	1	41.0	ruminant	1	50.0	7	0	N
Neotragus pygmaeus	Royal antelope	1	2.3	ruminant	0	0.0	7	0	N
Okapia johnstoni	Okapi	2	235.2	ruminant	1	0.0	7	0	N
Oreotragus oreotragus	Klipspringer	7	11.5	ruminant	0	1.0	1	0	N
Oryx beisa	East African oryx	8	168.6	ruminant	1	49.0	1	0	N
Oryx gazella	Gemsbok	24	203.7	ruminant	0	84.5	4	0	Y
Ourebia ourebi	Oribi	31	15.2	ruminant	0	43.5	1	0	Y
Pelea capreolus	Grey rhebok	6	22.0	ruminant	0	0.0	7	0	N
Phacochoerus africanus	Common warthog	48	75.9	non-ruminant	2	70.0	1	10	Y
Philantomba maxwellii	Maxwell's duiker	2	7.8	ruminant	0	0.0	1	10	N
Philantomba monticola	Blue duiker	6	4.8	ruminant	0	0.0	3	10	N
Potamochoerus porcus	Red river hog	8	66.6	non-ruminant	1	0.3	3	20	N
Raphicerus campestris	Steenbok	33	11.2	ruminant	0	14.0	4	0	Y
Raphicerus melanotis	Cape grysbok	2	10.3	ruminant	0	50.0	7	0	N
Raphicerus sharpei	Sharpe's grysbok	4	8.7	ruminant	0	50.0	7	0	N
Redunca arundinum	Southern reedbuck	30	53.5	ruminant	2	61.0	1	0	Y
Redunca fulvorufula	Mountain reedbuck	12	29.1	ruminant	2	96.5	4	0	N
Redunca redunca	Bohor reedbuck	22	46.9	ruminant	1	100.0	7	0	N
Sylvicapra grimmia	Common Duiker	56	16.9	ruminant	0	1.0	1	10	N
Syncerus caffer	African buffalo	74	486.3	ruminant	2	44.5	1	0	Y
Tragelaphus angasii	Nyala	5	85.7	ruminant	1	9.0	1	0	Y
Tragelaphus derbianus	Giant eland	7	598.2	ruminant	1	0.0	1	0	N
Tragelaphus eurycerus	Bongo	1	285.7	ruminant	2	0.0	3	0	N
Tragelaphus imberbis	Lesser kudu	7	86.3	ruminant	0	50.0	7	0	N
Tragelaphus oryx	Common eland	56	511.2	ruminant	0	8.5	1	0	N
Tragelaphus scriptus	Bushbuck	43	42.3	ruminant	1	5.0	2	0	Y
Tragelaphus spekii	Sitatunga	6	76.5	ruminant	2	17.0	4	0	N
Tragelaphus strepsiceros	Greater kudu	44	202.3	ruminant	1	0.5	1	0	Y

Table S5: Covariates used in generalized additive mixed-effect models (GAMMs) to predict large herbivore density.

Covariate	Mechanism	Data source details	Data source ref
Environmental factors			
NDVI	Forage quantity	MODIS/061/MOD13A2	Didan (2021)
Precipitation concentration index	Forage seasonality	WorldClim2	Fick and Hikmans (2017)
Soil fertility	Forage quality	iSDAsoil Fertility Capability Classification	Hengl et al. (2021)
Distance-to-water	Water availability	JRC Global Surface Water Mapping v1.4	Pekel et al. (2016)
Dietary sodium	Minimum sodium requirements	*This study*	*This study*
Anthropogenic factors			
Distance to nearest city	Accessibility for hunters/poachers to enter protected areas	Global Accessibility Indicators	Nelson et al. (2019)
Human development Index (HDI)	Less developed communities may facilitate more hunting of target herbivore species	Mean HDI 1990-2010	Smits and Permanyer (2019)
Hunting pressure	Anthropogenic impact: high hunting pressure can reduce herbivore density below ecological carrying capacity	Standardized proportion of species impacted by hunting	Harfoot et al. (2021)
Functional traits			
Body mass	Metabolic rate, energy demand	Published literature	Hempson et al. (2015)
Omnivory %	Additional source of nutrients	Published literature	Wilman et al. (2014)
Habitat preference	Forage, shelter, other habitat requirements	Published literature	Hempson et al. (2015)
Interactive effects			
Precipitation concentration index * Body mass	Fat stores, metabolic rate and body size	NA	Lindstedt and Boyce (1985)
Rural density * Body mass	Direct and indirect effects (e.g., hunting) are non-uniform across body size	NA	Fa et al. (2022)
Body mass * Dietary sodium	Larger animals more vulnerable to sodium deficiencies	NA	Duvall et al. (2023)
Latent effects			
Phylogenetic component 1	Latent phylogenetic effects not captured by functional traits	NA	*This study*
Phylogenetic component 2	Latent phylogenetic effects not captured by functional traits	NA	*This study*
Easting	Latent spatial effects not captured by environmental covariates	NA	*This study*
Northing	Latent spatial effects not captured by environmental covariates	NA	*This study*
Random effects			
Species	Species-specific effects not captured by functional traits	NA	*This study*
Region	Socio-economic and historical effects not captured in anthropic fixed effects	NA	*This study*

Table S6: Comparison of model performance of the base GAMM model during spatial-block, taxonomic-block and random-block cross validation using (i) all large herbivore density observations, and (ii) megaherbivores only. R^2 and root-mean squared error (RMSE) performance metrics represent the mean value across 10-folds or species, respectively, and are reported for both the training and test datasets. A large drop in performance metrics between training and test data indicates model overfitting. For inspection of the comparison between predicted and observed large herbivore densities during cross validation exercises, see Fig. S10. We did not perform phylogenetic-block cross validation on megaherbivores, as there were only four species included in this dataset.

Dataset	Cross validation	Training dataset		Test dataset	
		R^2	RMSE	R^2	RMSE
All herbivores (n=1170)	Spatial-block	0.38 ± 0.01	0.69 ± 0.01	0.20 ± 0.04	0.80 ± 0.08
	Phylogenetic-block	0.37 ± 0.01	0.69 ± 0.01	0.28 ± 0.25	0.84 ± 0.22
	Random-block	0.38 ± 0.01	0.69 ± 0.01	0.27 ± 0.03	0.76 ± 0.02
Megaherbivores only (n=135)	Spatial-block	0.50 ± 0.05	0.62 ± 0.02	0.27 ± 0.16	0.76 ± 0.19
	Phylogenetic-block	N/A	N/A	N/A	N/A
	Random-block	0.52 ± 0.07	0.61 ± 0.04	0.31 ± 0.16	0.74 ± 0.09

Table S7: Generalized additive mixed-effect model (GAMM) results for the best model predicting herbivore density, using all available observations. Results presented using as_flextable from the 'flextable' package (Gohl and Skintzos, 2023). Note: p-values of 0.0000 refer to p-values < 0.00001. For inspection of associated variable importance and partial dependence plots, see Fig. 3 and Extended Data Fig. 6, respectively.

Component	Term	Estimate	Std Error	t-value	p-value	
A. parametric coefficients	(Intercept)	-0.642	0.170	-3.787	0.0002	***
Component	**Term**	**edf**	**Ref. df**	**F-value**	**p-value**	
B. smooth terms	s(NDVI)	1.314	3.000	2.000	0.0190	*
	te(Precipitation_concentration_index,Log10_body_mass)	2.410	7.000	2.443	0.0013	**
	s(Soil_fertility)	0.953	2.000	12.026	0.0000	***
	s(Water_dist)	0.904	2.000	6.163	0.0004	***
	te(Diet_Na_selective,Log10_body_mass)	2.955	6.000	2.965	0.0136	*
	s(Habitat_preference)	1.318	2.000	12.639	0.0004	***
	s(Log10_body_mass)	0.000	3.000	0.000	0.3075	
	s(Omnivory_per)	0.000	2.000	0.000	0.4375	
	te(Hunting,Log10_body_mass)	2.197	6.000	3.150	0.0001	***
	s(Dist_to_city)	0.576	2.000	0.732	0.1070	
	s(HDI)	1.742	2.000	8.877	0.0001	***
	s(Phylogenetic_component_1)	0.587	2.000	19.506	0.1157	
	s(Phylogenetic_component_2)	0.000	2.000	0.000	0.7740	
	s(x,y)	3.761	34.000	0.725	0.0003	***
	s(Species)	37.593	63.000	3.336	0.0000	***
	s(Region)	2.777	3.000	15.528	0.0000	***

Signif. codes: 0 <= '***' < 0.001 < '**' < 0.01 < '*' < 0.05

Adjusted R-squared: 0.338, Deviance explained 0.371

fREML : 1331.600, Scale est: 0.508, N: 1170

Table S8: Generalized additive mixed-effect model (GAMM) results for the best model predicting megaherbivore density (elephant, giraffe, black rhino, white rhino). Results presented using as_flextable from the 'flextable' package (Gohl and Skintzos, 2023). Note: p-values of 0.0000 refer to p-values < 0.00001. For inspection of associated variable importance and partial dependence plots, see Fig. 3 and Extended Data Fig. 7, respectively.

Component	Term	Estimate	Std Error	t-value	p-value	
A. parametric coefficients	(Intercept)	-1.177	0.272	-4.322	0.0000	***
Component	**Term**	**edf**	**Ref. df**	**F-value**	**p-value**	
B. smooth terms	s(NDVI)	0.956	3.000	7.359	0.0000	***
	s(Precipitation_concentration_index)	0.000	2.000	0.000	0.2815	
	s(Soil_fertility)	0.779	2.000	3.337	0.0280	*
	s(Water_dist)	0.000	2.000	0.000	0.9872	
	s(Diet_Na_unselective)	0.860	2.000	3.383	0.0053	**
	s(Habitat_preference)	0.000	2.000	0.000	0.5552	
	s(Hunting)	0.826	2.000	2.480	0.0142	*
	s(Dist_to_city)	0.795	2.000	1.992	0.0241	*
	s(HDI)	1.315	2.000	2.407	0.0269	*
	s(x,y)	2.284	34.000	0.030	0.9163	
	s(Species)	2.734	3.000	15.382	0.0000	***
	s(Region)	0.000	3.000	0.000	0.2787	

Signif. codes: 0 <= '***' < 0.001 < '**' < 0.01 < '*' < 0.05

Adjusted R-squared: 0.455, Deviance explained 0.498

fREML : 146.476, Scale est: 0.419, N: 135

SUPPLEMENTARY FIGURES

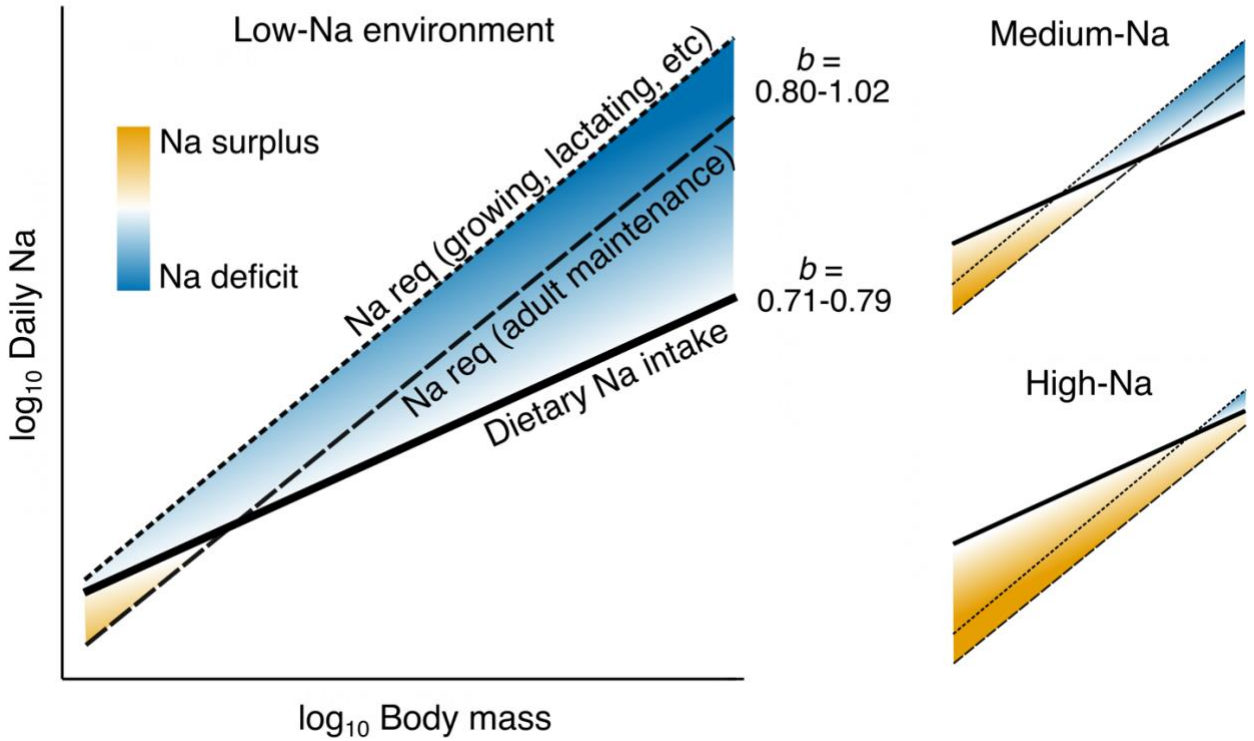

Figure S1. A conceptual figure showing theoretical drivers of sodium (Na) limitation in herbivorous mammals. Due to differences in the allometric scaling of Na requirements and dietary Na intake, large animals appear disproportionately more susceptible to Na limitation in Na-poor environments. Variable *b* represents the scaling a factor (slope) of the allometric relationship between body mass and Na requirement; it is steeper for requirement than intake, with growing or lactating individuals having a higher requirement value. The medium- and high-Na graphs highlight that as Na availability increases, different sized mammals will 'escape' Na deficit at different periods, with large mammals requiring higher Na availability. Recreated with permission from Duvall et al. (2023).

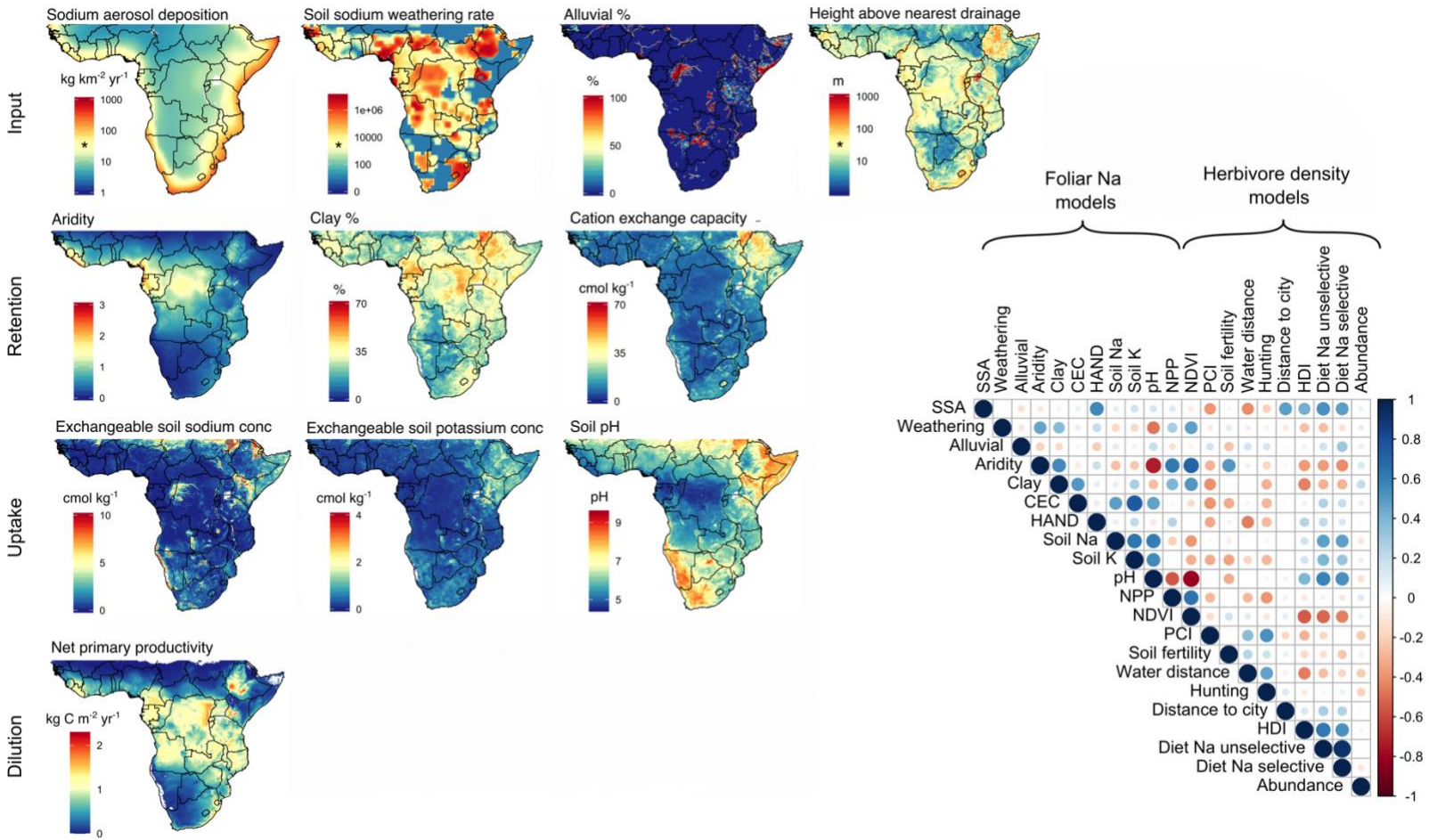

Figure S2a. Spatial mapping of predictor variables used to model foliar Na concentration across sub-Saharan Africa. Note: scales with * have been $\log_{10}$ transformed to better highlight regional differences. The scale for aridity is non-intuitive, with lower scores reflecting more arid environments (Trabucco and Zomer, 2018). We have grouped predictors based on their expected mechanistic impact on foliar Na concentrations (input, retention, uptake and dilution). A correlation matrix is included to highlight positive (blue) and negative (red) relationships between covariates. Note: this correlation matrix also includes variables used to model large-herbivore density to check for potential issues of "double counting".

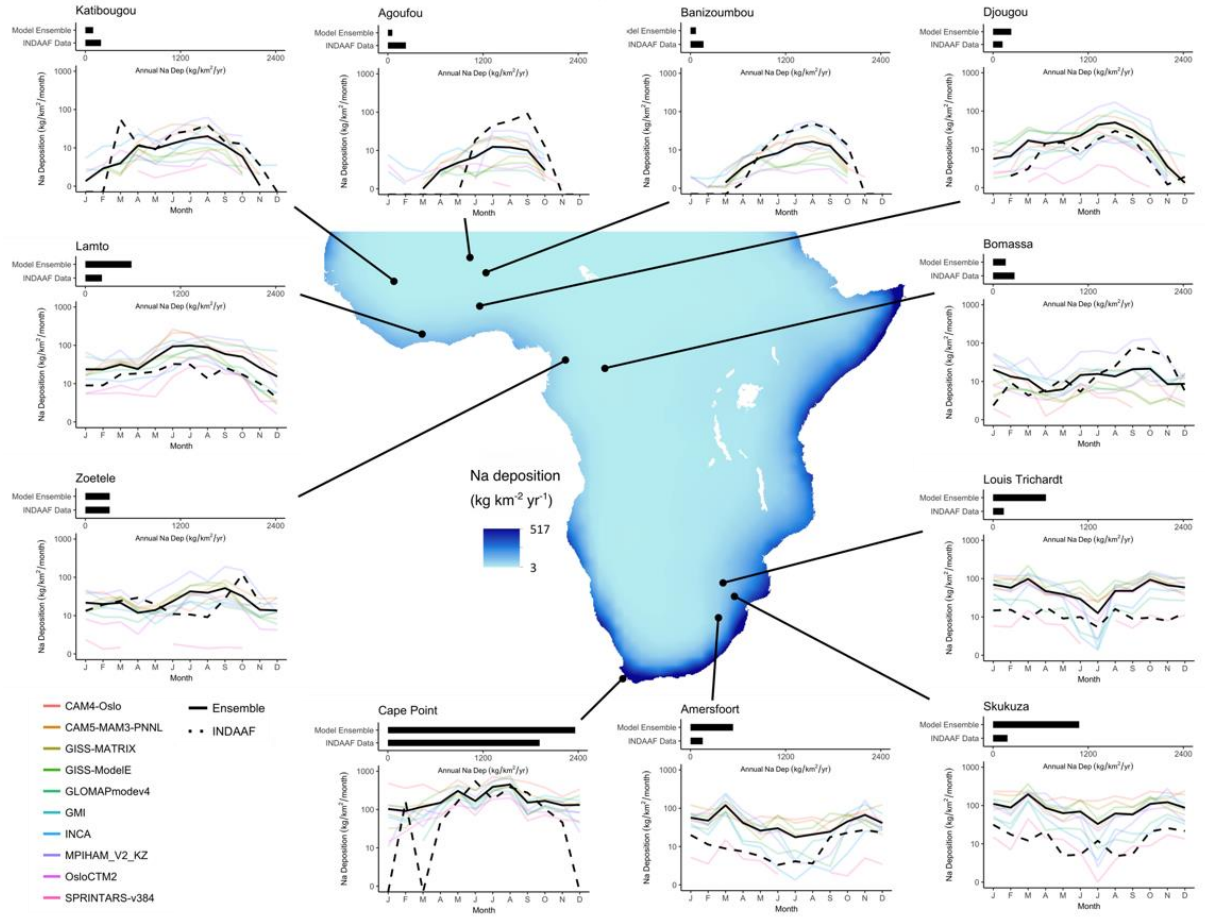

Figure S2b. Validation of sodium (Na) aerosol deposition model used in Fig S3a, which was generated as the mean from 10 separate aerosol models within the AeroCom database (https://aerocom.met.no/Welcome.html; see text S1 for methodological details). Inset graphs compare model predictions with annual and monthly measured wet deposition of sodium at 11 International Network to study Deposition and Atmospheric chemistry in Africa (INDAAF) sites (https://indaaf.obs-mip.fr/network/) distributed across sub-Saharan Africa.

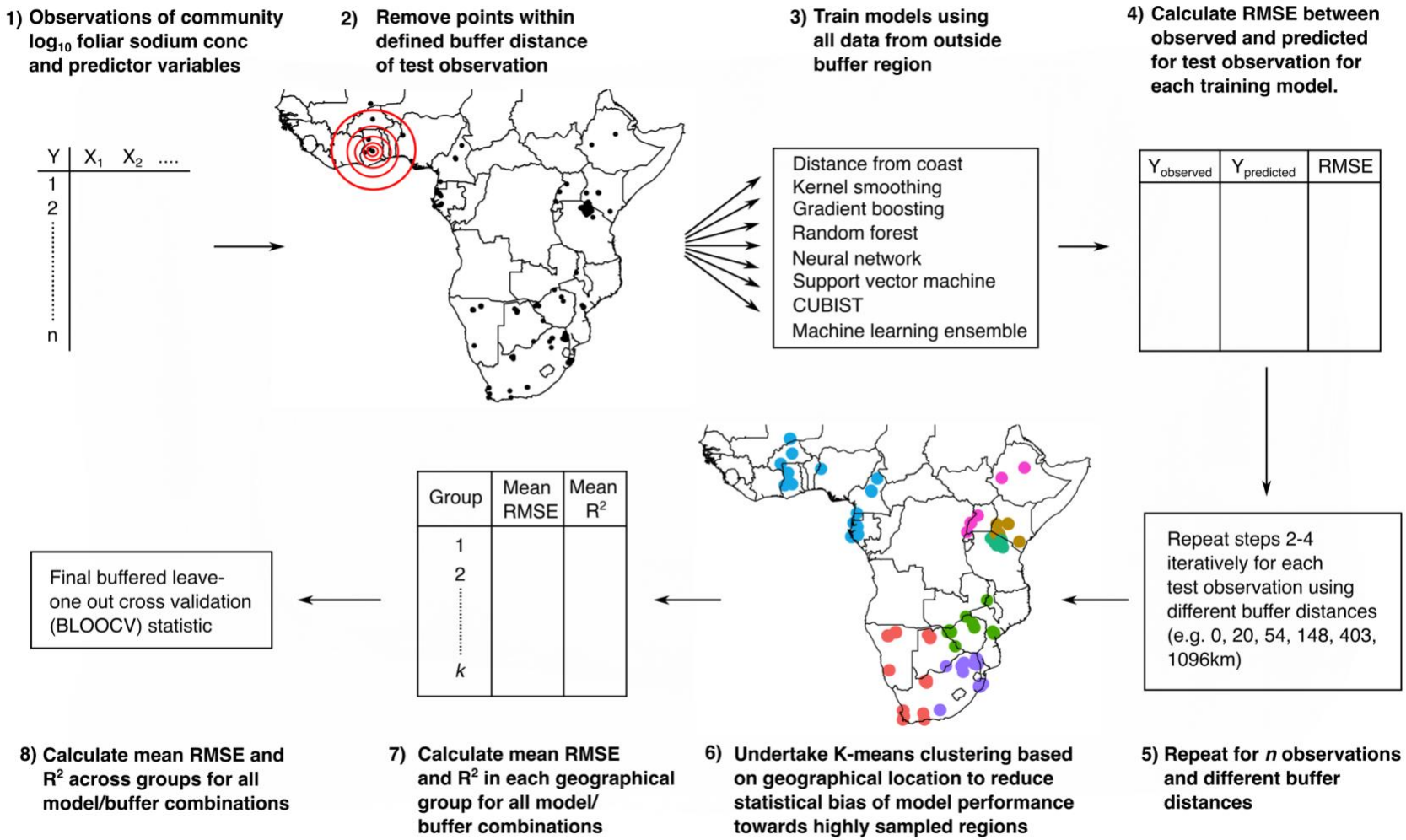

Figure S3. Workflow to perform buffered leave-one-out cross validation (BLOOCV) for foliar median and 95th percentile Na concentration prediction models. For the K-means clustering, 7 clusters were chosen based on the elbow method. Model RMSE refers to root mean squared error.

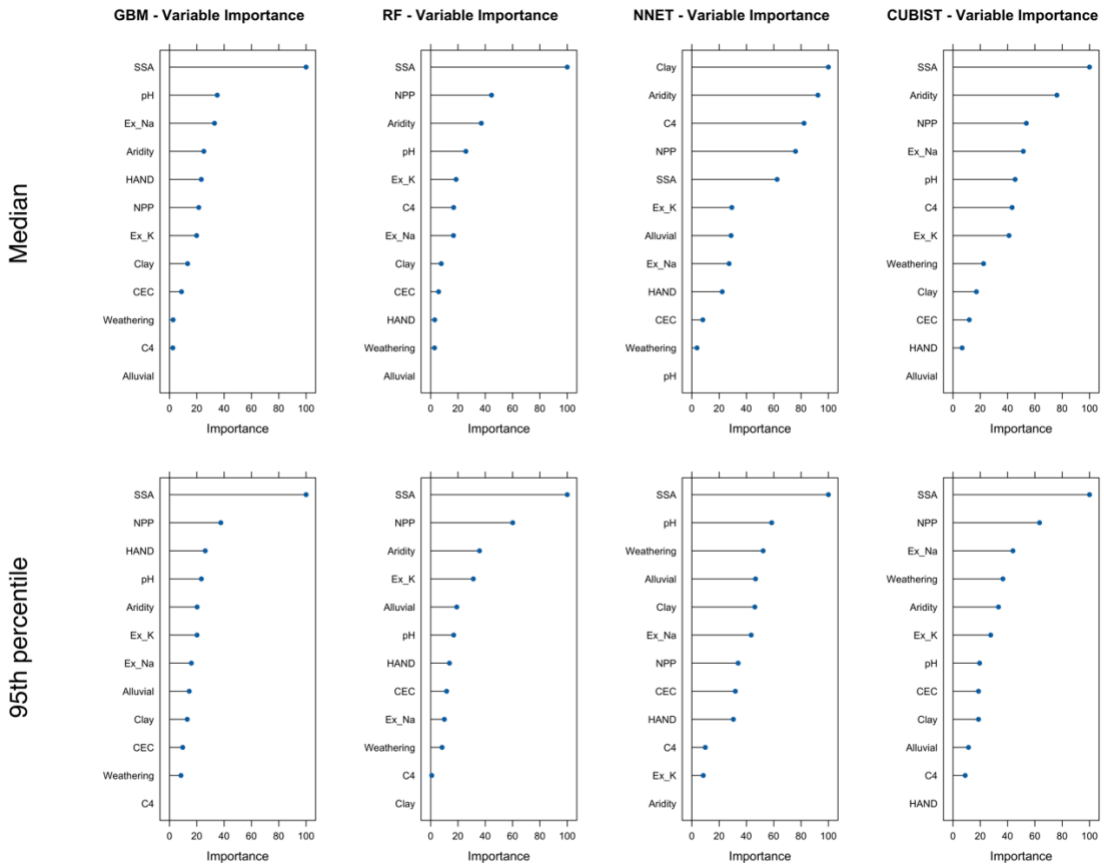

Figure S4. Variable importance plots for predicting foliar median and 95th percentile sodium concentration using gradient boosted (GBM), random forest (RF), neural network (NNET) and cubist (CUBIST) models. Note there is no variable importance plot for the support vector machine (SVM) or ensemble model as the '*caret*' package does not support this function. Alluvial – alluvial %; Aridity – aridity index; CEC – cation exchange capacity; Clay – soil clay fraction; Ex_K – exchangeable soil K; Ex_Na – exchangeable soil Na; HAND – height above nearest drainage; MAP – mean annual precipitation; NPP – net primary productivity; pH – soil pH; SSA - sea salt aerosol deposition; Weathering – rock sodium weathering rate. Some variables (e.g., alluvial %) feature with low importance at the continental-scale, but are likely more important at local scales.

MEDIAN scenario

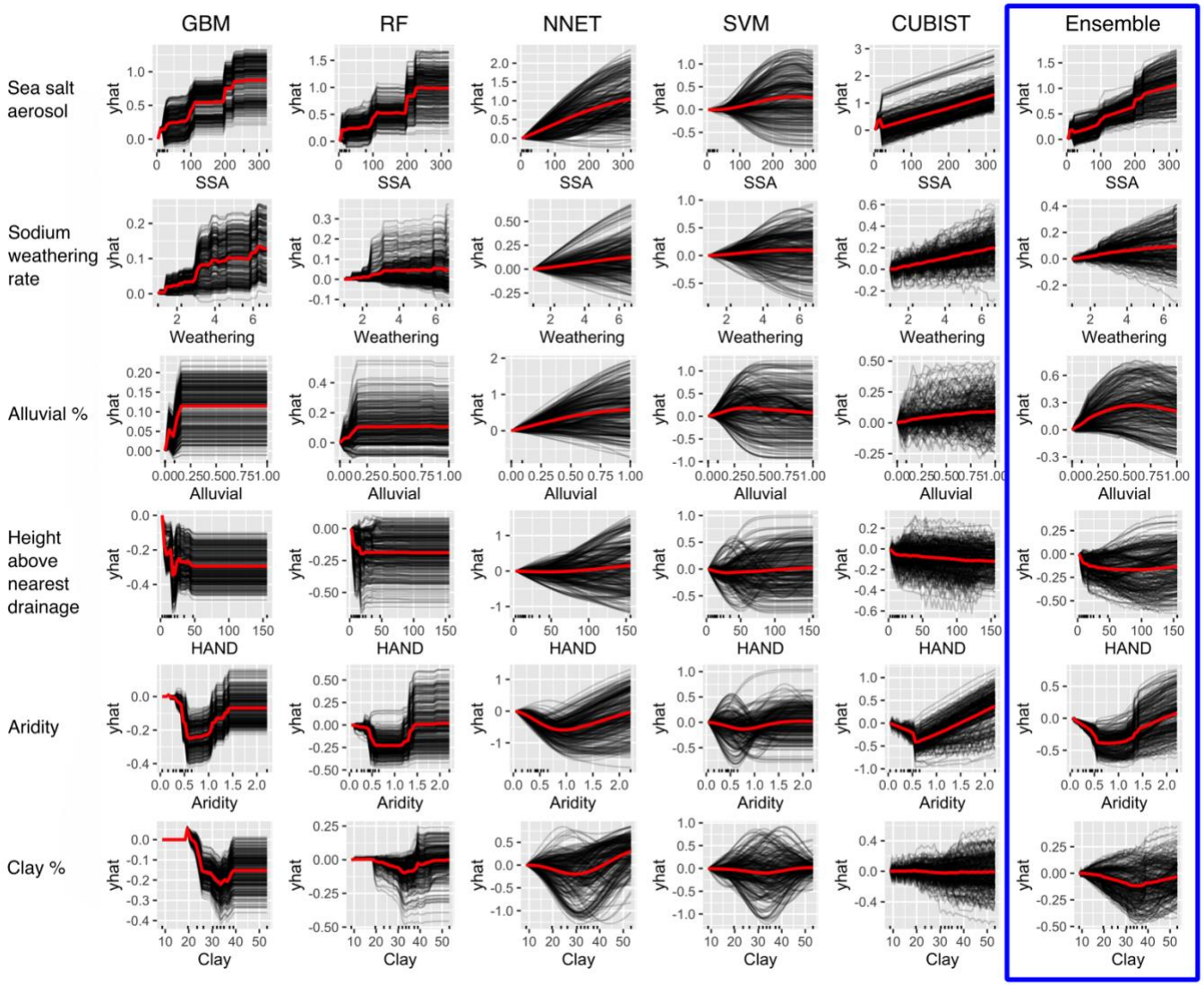

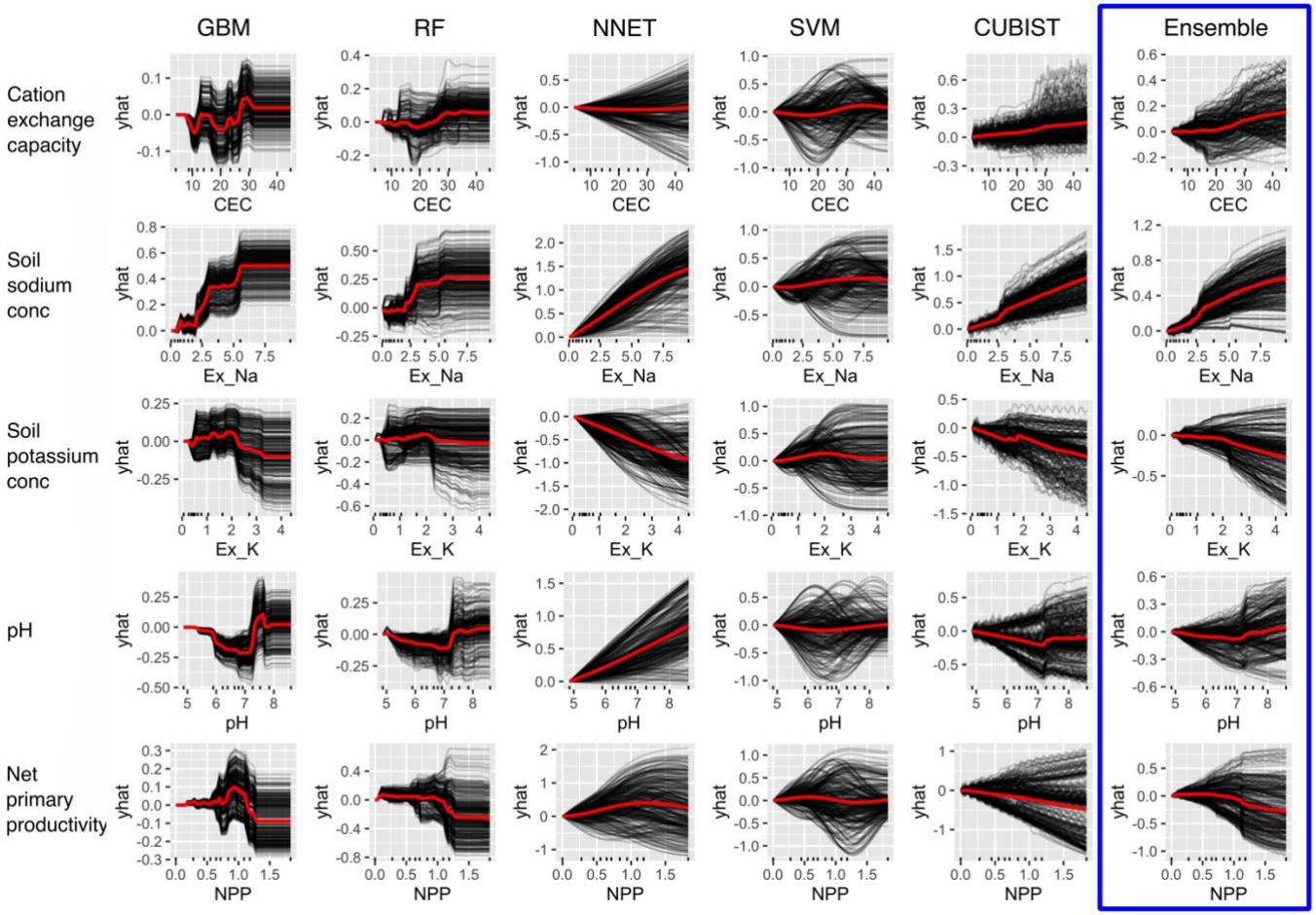

Figure S5. Partial dependence plots for predicting foliar community median sodium concentration using gradient boosted (GBM), random forest (RF), neural network (NNET), support vector machine (SVM), cubist (CUBIST) and ensemble models generated in this study. The relationship between foliar sodium concentration and each variable in the ensemble model is highlighted within the blue box. Note: the scale for aridity is non-intuitive, with lower scores reflecting more arid environments (Trabucco and Zomer, 2018).

95th PERCENTILE scenario

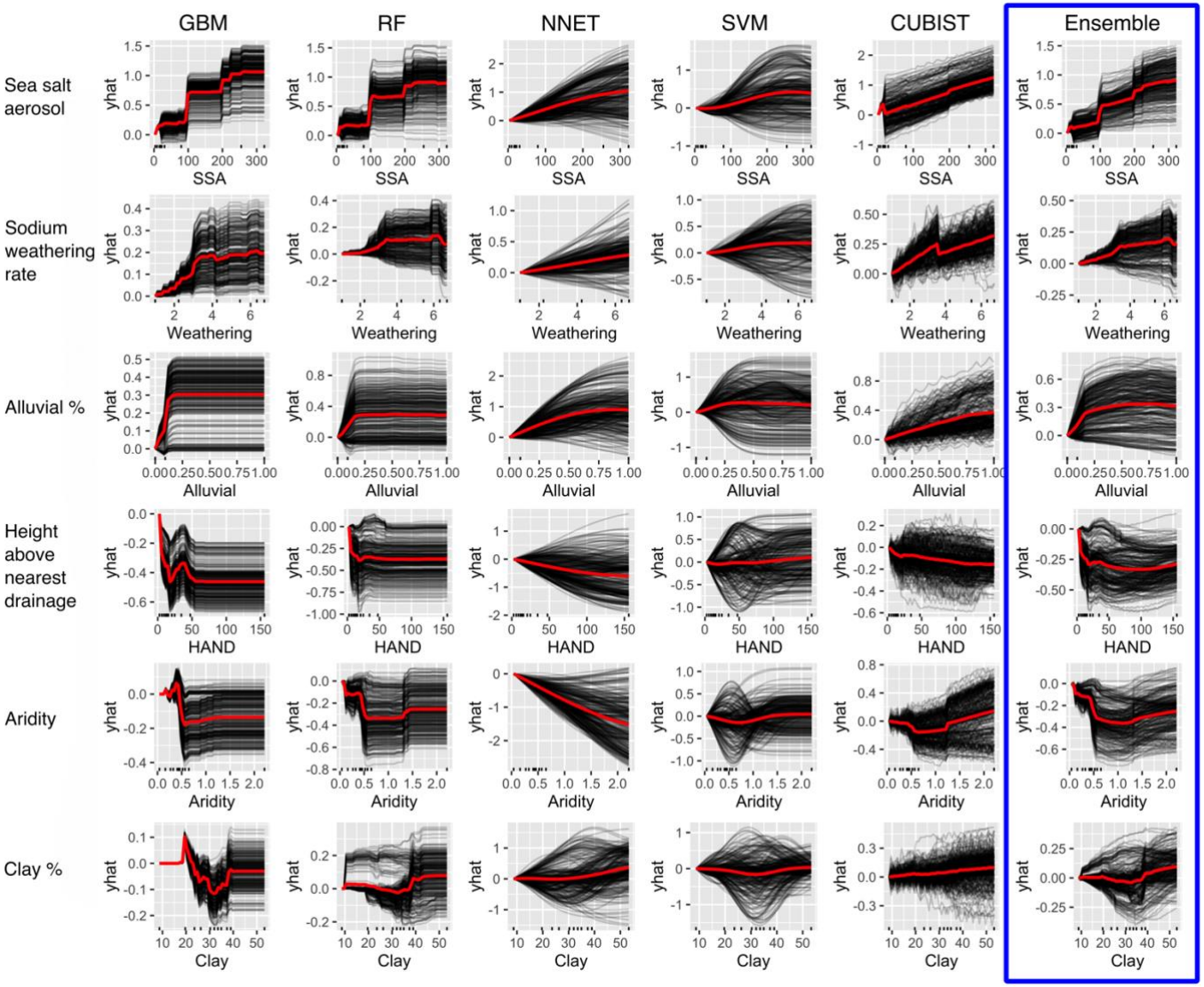

95th PERCENTILE scenario (*ctd.*)

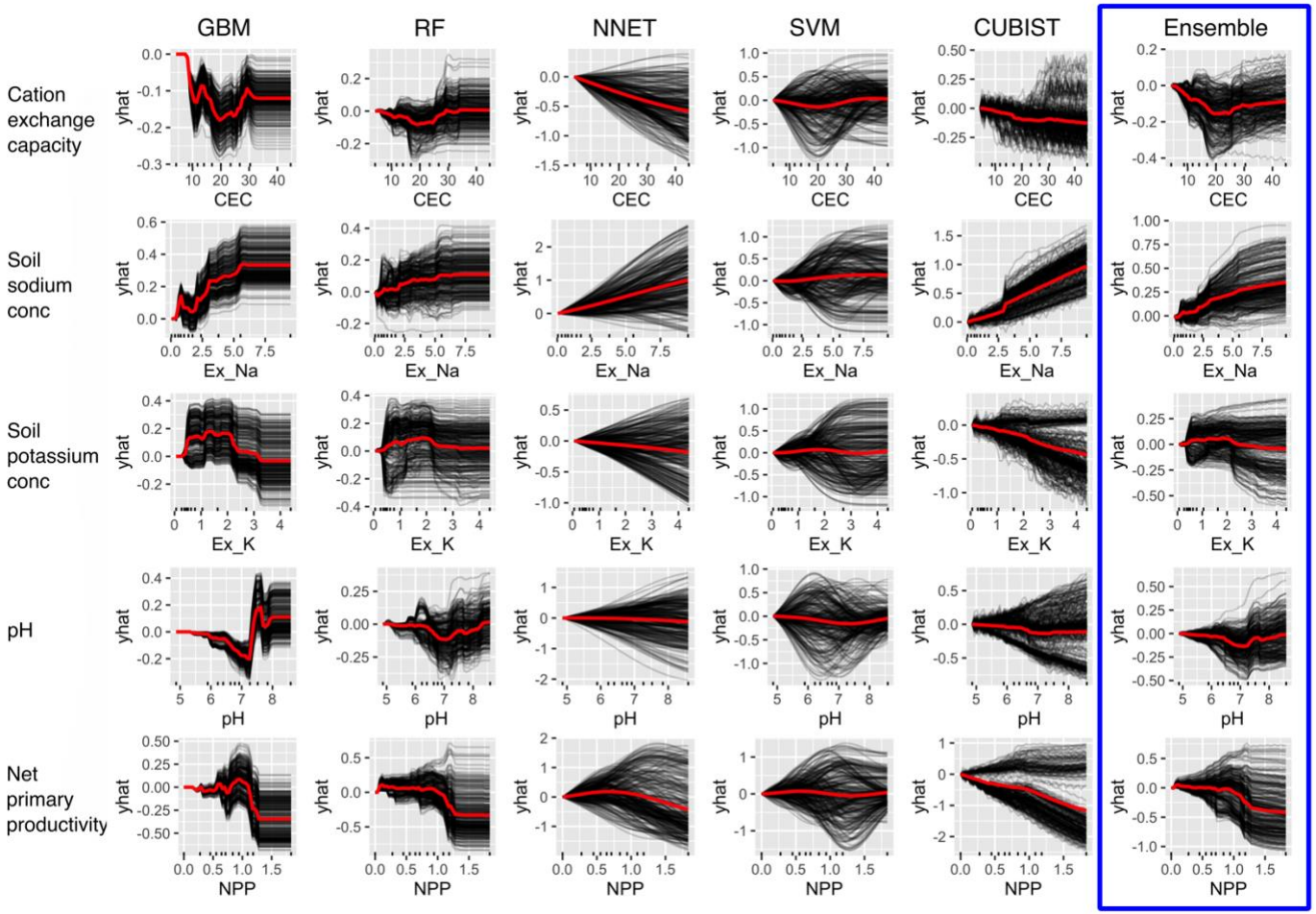

Figure S6. Partial dependence plots for predicting foliar community 95th percentile sodium concentration using gradient boosted (GBM), random forest (RF), neural network (NNET), support vector machine (SVM), cubist (CUBIST) and ensemble models generated in this study. The relationship between foliar sodium concentration and each variable in the ensemble model is highlighted within the blue box. Note: the scale for aridity is non-intuitive, with lower scores reflecting more arid environments (Trabucco and Zomer, 2018).

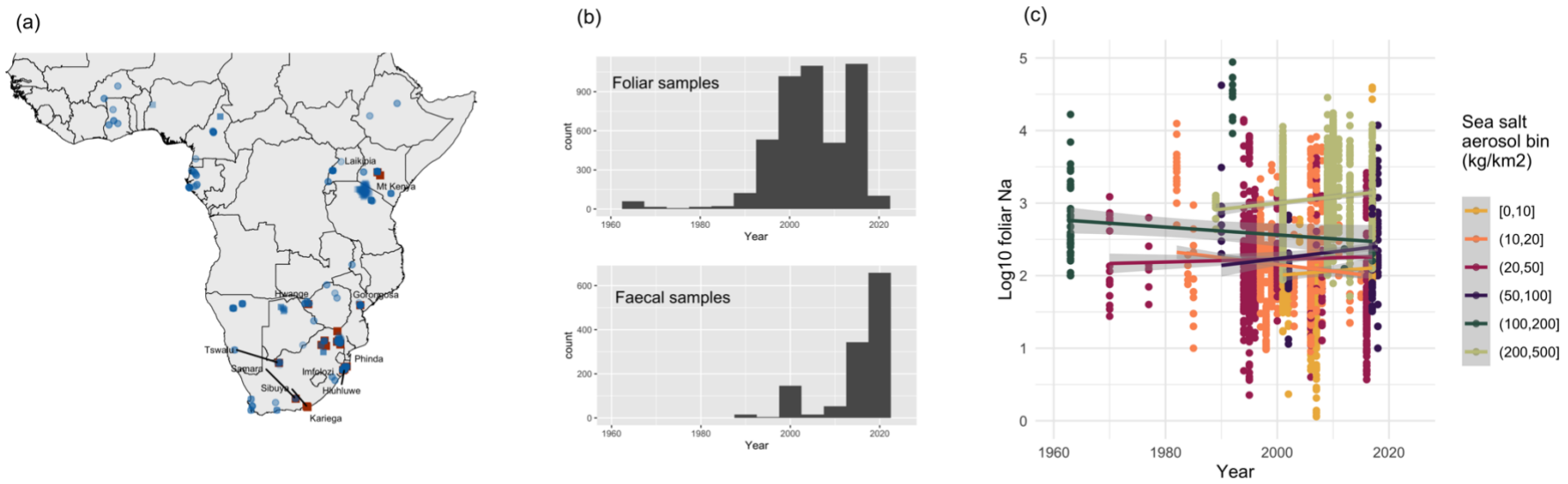

Figure S7. (a) Spatial mapping of large-herbivore faecal samples (brown points); plant samples are mapped (blue points) to show levels of congruence between faecal and plant measurements. (b) Histogram of sample collection for foliar and faecal samples analysed in this study highlighting that faecal samples have generally been collected more recently (2000-2022) than foliar samples (1960-2022). Due to the potential issues of climate change induced nutrient dilution (sensus Kaspari and Welti, 2025) this may lead to incongruities between modelled estimates of foliar sodium (Na) and observed faecal samples presented in Fig. 2 and Extended Data Fig. 5. (c) Assessment of foliar Na concentrations through time binned got different regions of sea salt aerosol deposition indicate that the majority of the variance is explained by spatial and physiological factors (n=4,619 in 289 independent geographical locations). Error bars equal 95% confidence intervals. While time does not appear to be the primary determinant of foliar Na (i.e., there is not a consistent pattern of decreasing foliar Na within each region), we do note, that more rigorous analysis may elucidate temporal patterns related to nutrient dilution.

Figure S8. Locations of herbivore density data from Hempson et al. (2015) used to build generalised additive models. 'Species n' refers to number of different species recorded at that site.

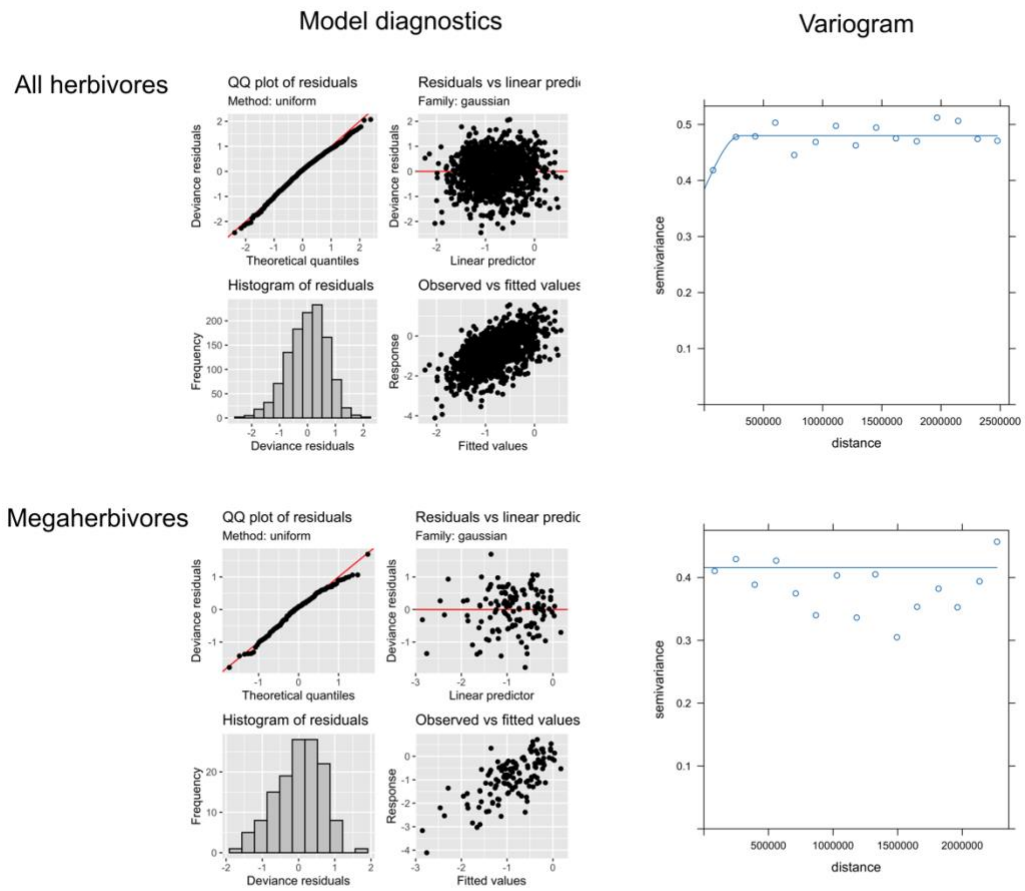

Figure S9. Model diagnostics and variogram plots for generalized additive mixed models (GAMMs) predicting density for (i) all herbivores, and (ii) megaherbivores only. There are no deviations from model assumptions and models do not contain spatial autocorrelation.

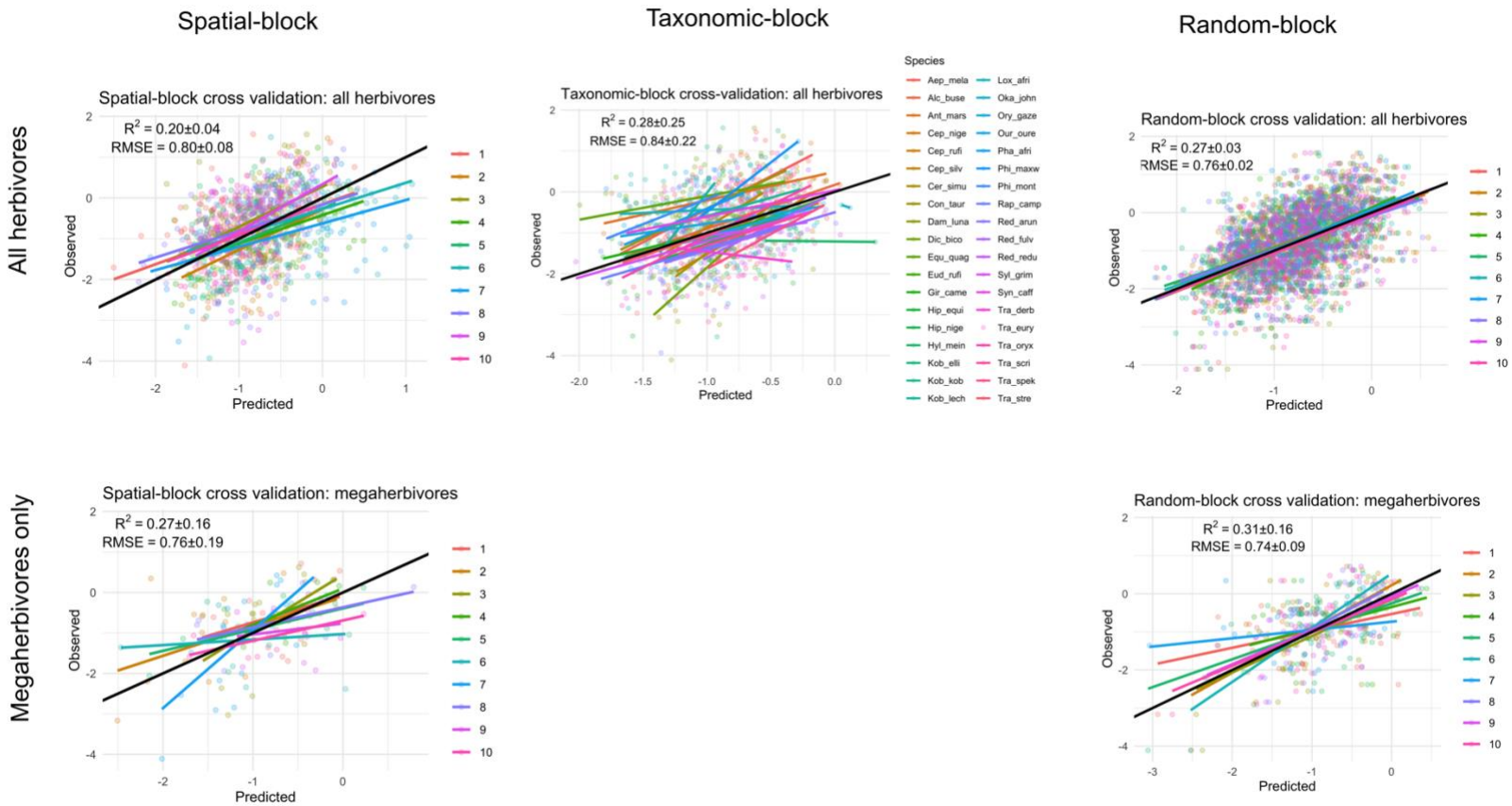

Figure S10. Comparison of predicted and observed large herbivore density in spatial-block, taxonomic-block and random-block cross validation for the base GAMM using all large herbivore density observations (n=1170; top row), and megaherbivore-species only (n=135; bottom row). The black line represents a 1:1 line. The linear fit between predicted and observed densities is highlighted for each fold/species separately. Predictive performance is highlighted in each plot using the mean ± standard deviation for R^2 and the root mean squared error (RMSE) across folds and species, respectively. RMSE values are $\log_{10}$ units.

REFERENCES

Adon, M., Galy-Lacaux, C., Delon, C., Yoboue, V., Solmon, F., & Kaptue Tchuente, A. T. (2013). Dry deposition of nitrogen compounds (NO 2, HNO 3, NH 3), sulfur dioxide and ozone in west and central African ecosystems using the inferential method. *Atmospheric Chemistry and Physics*, *13*(22), 11351-11374.

Bell, R. H. V. The Effect of Soil Nutrient Availability on Community Structure in African Ecosystems. in *Ecology of Tropical Savannas* (eds. Huntley, B. J. & Walker, B. H.) 193–216 (Springer, Berlin, Heidelberg, 1982). doi:10.1007/978-3-642-68786-0_10.

Borer, E. T., Lind, E. M., Firn, J., Seabloom, E. W., Anderson, T. M., Bakker, E. S., ... & Stevens, C. J. (2019). More salt, please: global patterns, responses and impacts of foliar sodium in grasslands. *Ecology Letters*, *22*(7), 1136-1144.

Cerling, T. E., Harris, J. M., & Passey, B. H. (2003). Diets of East African Bovidae based on stable isotope analysis. *Journal of Mammalogy*, *84*(2), 456-470.

Clay, N. A., Lehrter, R. J., & Kaspari, M. (2017). Towards a geography of omnivory: Omnivores increase carnivory when sodium is limiting. *Journal of Animal Ecology*, *86*(6), 1523-1531.

Codron, D., Codron, J., Lee-Thorp, J. A., Sponheimer, M., De Ruiter, D., Sealy, J., ... & Fourie, N. (2007). Diets of savanna ungulates from stable carbon isotope composition of faeces. *Journal of Zoology*, *273*(1), 21-29.

Coe, M. J., Cumming, D. H. & Phillipson, J. (1976). Biomass and production of large African herbivores in relation to rainfall and primary production. *Oecologia,* 22, 341-354.

Cooney, R., Roe, D., Dublin, H., Phelps, J., Wilkie, D., Keane, A., Travers, H., Skinner, D., & Challender, D. W. S. (2016). From poachers to protectors: Engaging local communities in solutions to illegal wildlife trade. *Conservation Letters, 10*(3), 367-374. https://doi.org/10.1111/conl.12294

Critchlow, R., Plumptre, A. J., Driciru, M., Rwetsiba, A., Stokes, E. J., Tumwesigye, C., Wanyama, F., & Beale, C. M. (2015). Spatiotemporal trends of illegal activities from ranger-collected data in a Ugandan national park. *Conservation Biology*, *29*(5), 1458-1470.

Daskin, J. H., & Pringle, R. M. (2018). Warfare and wildlife declines in Africa's protected areas. *Nature*, *553*(7688), 328-332.

Didan, K. (2021). *MODIS/Terra Vegetation Indices 16-Day L3 Global 1km SIN Grid V061* [Data set]. NASA EOSDIS Land Processes Distributed Active Archive Center. Accessed 2023-11-09 from https://doi.org/10.5067/MODIS/MOD13A2.061

Donchyts, G., Winsemius, H., Schellekens, J., Erickson, T., Gao, H., Savenije, H., & van de Giesen, N. (2016). Global 30m height above the nearest drainage. *HAND*, *1000*(0).

Dorgeloh, W. G., Van Hoven, W & Rethman, N. F. G. (1998). Faecal analysis as an indicator of the nutritional status of the diet of roan antelope in South Africa. *South African Journal of Wildlife*, *28*(1), 16-21.

Duffy, R., & St John, F. (2013). Poverty, Poaching and Trafficking: What are the links? In *A report for the UK Department for International Development (DFID)* (Issue June). https://doi.org/10.12774/eod_hd059.jun2013.duffy

Duvall, E. S., Griffiths, B. M., Clauss, M., & Abraham, A. J. (2023). Allometry of sodium requirements and mineral lick use among herbivorous mammals. *Oikos*, *2023*(9), e10058.

East, R. (1984). Rainfall, soil nutrient status and biomass of large African savanna mammals. *African Journal of Ecology, 22*, 245-270.

Fa, J. E., & Brown, D. (2009). Impacts of hunting on mammals in African tropical moist forests: a review and synthesis. *Mammal Review*, *39*(4), 231-264.

Fa, J. E., Funk, S. M., & Nasi, R. (2022). Hunting wildlife in the tropics and subtropics. Cambridge University Press.

Faurby, S., Davis, M., Pedersen, R. Ø., Schowanek, S. D., Antonelli, A., & Svenning, J. C. (2018). PHYLACINE 1.2: the phylogenetic atlas of mammal macroecology. *Ecology*, *99*(11), 2626.

Fick, S. E., & Hijmans, R. J. (2017). WorldClim 2: new 1-km spatial resolution climate surfaces for global land areas. *International Journal of Climatology*, *37*(12), 4302-4315.

Fritz, H. & Duncan, P. (1997). On the carrying capacity for large ungulates of African savanna ecosystems. *Proceedings of the Royal Society of London B Biological Sciences, 256*(1345), 77-82.

Gagnon, M., & Chew, A. E. (2000). Dietary preferences in extant African Bovidae. *Journal of Mammalogy*, *81*(2), 490-511.

Gaillardet, J., Dupré, B., Louvat, P., & Allegre, C. J. (1999). Global silicate weathering and CO2 consumption rates deduced from the chemistry of large rivers. *Chemical Geology*, *159*(1-4), 3-30.

Gaynor, K. M., Fiorella, K. J., Gregory, G. H., Kurz, D. J., Seto, K. L., Withey, L. S., & Brashares, J. S. (2016). War and wildlife: linking armed conflict to conservation. *Frontiers in Ecology and the Environment*, *14*(10), 533-542. https://doi.org/10.1002/fee.1433

Gohel D, Skintzos P (2023). _flextable: Functions for Tabular Reporting_. R package version 0.9.4, <https://CRAN.R-project.org/package=flextable>.

Harfoot, M. B., Johnston, A., Balmford, A., Burgess, N. D., Butchart, S. H., Dias, M. P., ... & Geldmann, J. (2021). Using the IUCN Red List to map threats to terrestrial vertebrates at global scale. *Nature Ecology & Evolution*, *5*(11), 1510-1519.

Harris, I. P. D. J., Jones, P. D., Osborn, T. J., & Lister, D. H. (2014). Updated high-resolution grids of monthly climatic observations–the CRU TS3. 10 Dataset. *International Journal of Climatology*, *34*(3), 623-642.

Hengl, T., Heuvelink, G. B., Kempen, B., Leenaars, J. G., Walsh, M. G., Shepherd, K. D., ... & Tondoh, J. E. (2015). Mapping soil properties of Africa at 250 m resolution: Random forests significantly improve current predictions. *PLoS One*, *10*(6), e0125814.

Hengl, T., Miller, M. A., Križan, J., Shepherd, K. D., Sila, A., Kilibarda, M., ... & Crouch, J. (2021). African soil properties and nutrients mapped at 30 m spatial resolution using two-scale ensemble machine learning. *Scientific Reports, 11*(1), 6130.

Holdø, R. M., Dudley, J. P., & McDowell, L. R. (2002). Geophagy in the African elephant in relation to availability of dietary sodium. *Journal of Mammalogy*, *83*(3), 652-664.

Kalumanga, E., Mpanduji, D. G., & Cousins, S. A. O. (2017). Geophagic termite mounds as one of the resources for African elephants in Ugalla Game Reserve, Western Tanzania. *African Journal of Ecology, 55*(1), 91-100.

Kartzinel, T. R., & Pringle, R. M. (2020). Multiple dimensions of dietary diversity in large mammalian herbivores. *Journal of Animal Ecology*, *89*(6), 1482-1496.

Kaspari, M. & Welti, E. A. R. Nutrient dilution and the future of herbivore populations. *Trends Ecol. Evol.* **0**, (2024).

Kattge, J., Bönisch, G., Díaz, S., Lavorel, S., Prentice, I. C., Leadley, P., ... & Cuntz, M. (2020). TRY plant trait database–enhanced coverage and open access. *Global Change Biology*, *26*(1), 119-188.

Kaufmann, D., Kraay, A., & Mastruzzi, M. (2011). The Worldwide Governance Indicators: Methodology and analytical issues. *Hague Journal on the Rule of Law*, *3*(2), 220-246.

Kennedy, C.M., Oakleaf, J.R., Theobald, D.M., Baurch-Murdo, S., & Kiesecker, J. (2019). Managing the middle: A shift in conservation priorities based on the global human modification gradient. *Global Change Biology, 25*(3), 811-826.

Lindstedt, S. L., & Boyce, M. S. (1985). Seasonality, fasting endurance, and body size in mammals. *The American Naturalist*, *125*(6), 873-878.

Macandza, V., Owen-Smith, N., & Le Roux, E. (2014). Faecal nutritional indicators in relation to the comparative population performance of sable antelope and other grazers. *African Journal of Ecology*, *52*(3), 300-307.

Mahaney, W. C., & Hancock, R. G. V. (1990). Geochemical analysis of African buffalo geophagic sites and dung on Mount Kenya, East Africa. *Mammalia*, *54*(1), 25-32.

Nelson, A., Weiss, D. J., van Etten, J., Cattaneo, A., McMenomy, T. S., & Koo, J. (2019). A suite of global accessibility indicators. *Scientific Data*, *6*(1), 266.

Osborne, C.P., Salomaa, A., Kluyver, T.A., Visser, V., Kellogg, E.A., Morrone, O., Vorontsova, M.S., Clayton, W.D. and Simpson, D.A. (2014) A global database of C4 photosynthesis in grasses. *New Phytologist, 204*(3), 441-446.

Pansu, J., Hutchinson, M. C., Anderson, T. M., Te Beest, M., Begg, C. M., Begg, K. S., ... & Pringle, R. M. (2022). The generality of cryptic dietary niche differences in diverse large-herbivore assemblages. *Proceedings of the National Academy of Sciences*, *119*(35), e2204400119.

Pekel, J.-F., Cottam, A., Gorelick, N., & Belward, A. S. (2016). High-resolution mapping of global surface water and its long-term changes. *Nature, 540*(7633), 418-422.

Pranzini, N., Maiorano, L., Cosentino, F., Thuiller, W., & Santini, L. (2024). The role of species interactions in shaping the geographic pattern of ungulate abundance across African savannah. *Scientific Reports*, *14*(1), 19647.

Roberts, D. R., Bahn, V., Ciuti, S., Boyce, M. S., Elith, J., Guillera-Arroita, G., ... & Dormann, C. F. (2017). Cross-validation strategies for data with temporal, spatial, hierarchical, or phylogenetic structure. *Ecography, 40*(8), 913-929.

Rothman, J. M., Van Soest, P. J., & Pell, A. N. (2006). Decaying wood is a sodium source for mountain gorillas. *Biology Letters*, *2*(3), 321-324.

Sach, F., Yon, L., Henley, M. D., Bedetti, A., Buss, P., de Boer, W. F., ... & Watts, M. J. (2020). Spatial geochemistry influences the home range of elephants. *Science of the Total Environment*, *729*, 139066.

Sayre, R., Comer, P., Hak, J., Josse, C., Bow, J., Warner, H., ... & Waruingi, L. (2013). A new map of standardized terrestrial ecosystems of Africa. *African Geographical Review*, 1-24.

Schlossberg, S., Gobush, K. S., Chase, M. J., Elkan, P. W., Grossmann, F., & Kohi, E. M. (2020). Understanding the drivers of mortality in African savannah elephants. *Ecological Applications*, *30*(6), 1-15.

Smith, R. J., Muir, R. D. J., Walpole, M. J., Balmford, A., & Leader-Williams, N. (2003). Governance and the loss of biodiversity. *Nature*, *426*(6962), 67-70.

Smits, J., & Permanyer, I. (2019). Data descriptor: The subnational human development database. *Scientific Data*, *6*, 1-15.

Sponheimer, M., Lee-Thorp, J. A., DeRuiter, D. J., Smith, J. M., Van Der Merwe, N. J., Reed, K., ... & Marcus, W. (2003). Diets of southern African Bovidae: stable isotope evidence. *Journal of Mammalogy*, *84*(2), 471-479.

Taylor, L. L., Quirk, J., Thorley, R. M., Kharecha, P. A., Hansen, J., Ridgwell, A., ... & Beerling, D. J. (2016). Enhanced weathering strategies for stabilizing climate and averting ocean acidification. *Nature Climate Change*, *6*(4), 402-406.

Trabucco, A., & Zomer, R. J. (2018). Global aridity index and potential evapotranspiration (ET0) climate database v2. *CGIAR Consort Spat Inf*.

Tracy, B. F., & McNaughton, S. J. (1995). Elemental analysis of mineral lick soils from the Serengeti National Park, the Konza Prairie and Yellowstone National Park. *Ecography*, *18*(1), 91-94.

Tsigaridis, K., Daskalakis, N., Kanakidou, M., Adams, P. J., Artaxo, P., Bahadur, R., ... & Zhang, X. (2014). The AeroCom evaluation and intercomparison of organic aerosol in global models. *Atmospheric Chemistry and Physics*, *14*(19), 10845-10895.

Western, D. (1975). Water availability and its influence on the structure and dynamics of a savannah large mammal community. *African Journal of Ecology*, *13*(3-4), 265-286.

White, F. The Vegetation of Africa; a descriptive memoir to accompany the UNESCO/AETFAT/UNSO vegetation map of Africa. https://unesdoc.unesco.org/ark:/48223/pf0000058054 (1983).

Wilman, H., Belmaker, J., Simpson, J., de la Rosa, C., Rivadeneira, M. M., & Jetz, W. (2014). EltonTraits 1.0: Species-level foraging attributes of the world's birds and mammals: Ecological Archives E095-178. *Ecology*, *95*(7), 2027.

Woodward, F. I., & Lomas, M. R. (2004). Vegetation dynamics–simulating responses to climatic change. *Biological reviews*, *79*(3), 643-670.

Vet, R., Artz, R. S., Carou, S., Shaw, M., Ro, C. U., Aas, W., ... & Reid, N. W. (2014). A global assessment of precipitation chemistry and deposition of sulfur, nitrogen, sea salt, base cations, organic acids, acidity and pH, and phosphorus. *Atmospheric Environment*, *93*, 3-100.

Vogel, S. M., Blumenthal, S. A., de Boer, W. F., Masake, M., Newton, I., Songhurst, A. C., ... & Coulson, T. (2020). Timing of dietary switching by savannah elephants in relation to crop consumption. *Biological Conservation*, *249*, 108703.

Yoganand, K., & Owen-Smith, N. (2014). Restricted habitat use by an African savanna herbivore through the seasonal cycle: key resources concept expanded. *Ecography*, *37*(10), 969-982.

Zhang, L., & He, Z. (2014). An empirical algorithm estimating dry deposition velocity of fine, coarse and giant particles. *Atmospheric Chemistry and Physics*, *14*(7), 3729-3737.